TABLE 5
Observed and Fitted Background and Excess Cases of Acute Myeloid Leukemia by Weighted Bone Marrow Dose Category

Dose (Gy)	Person years	Observed cases	Fitted cases†	
			Background	Excess
<0.005	2,039,093	77	75.6	0.0
–0.1	957,889	36	37.7	0.2
–0.2	201,935	9	8.2	0.6
–0.5	206,749	12	8.4	2.7
–1	117,855	11	4.9	6.9
–2	64,122	18	2.8	14.0
2+	25,761	13	1.0	13.0
Total	3,613,404	176	138.6	37.4

† Estimates based on the preferred quadratic ERR model described in the text and Table 6 with additional details in supplementary Table S2 (http://dx.doi.org/10.1667/RR2892.1.S1).

current model together with using lighter lines, the pattern from an EAR model of the form used in the 1994 report. The new model predicts somewhat lower excess rates shortly after the bombings for those exposed as children, and somewhat higher rates throughout the follow-up for those exposed at age 50.

The fitted models illustrated in Fig. 2f reveal an upward trend in the AML excess rates in recent years, suggesting that excess risks have persisted throughout the entire follow-up period. Categorical analyses based on a simple model with main effects for three age-at-exposure and six period effects were used to assess the persistence of the risk. As seen in Table 7, there was evidence of increased risks in the last 12 years of follow-up with a significantly elevated ERR at 1 Gy of 1.5, representing about 6 excess cases during this period.

Acute Lymphoblastic Leukemia (ALL)

There were 43 eligible ALL cases. This relatively small number of cases, coupled with a large proportion (about half, described below) being associated with radiation exposure, makes it difficult to make precise inferences about the baseline rates. However, it appeared that ALL baseline rates increased with attained age ($P = 0.01$). This increase was estimated to be proportional to attained age to the power 1.70 (95% CI 0.34–3.36) (supplementary Table S2; http://dx.doi.org/10.1667/RR2892.1.S1), and allowing for more complex age patterns did not improve the fit. Population data for Japan and other countries (*34*) suggest that ALL baseline rates have a U-shaped pattern in which the rates reach a minimum in the 30–40 age range and increase at older ages. We did not find evidence for such a pattern in our data, most likely reflects the limited power due to the small number of cases in the cohort. There was no evidence of gender differences in either the level of risk ($P > 0.5$) or the age pattern ($P > 0.5$), nor were there any indications of a trend in the baseline rates with birth cohort ($P = 0.17$) or of city differences ($P = 0.43$). Figure 3a illustrates how the fitted baseline ALL rates vary with attained age. The ALL baseline rate model and parameter estimates are given in supplementary Table S2 (http://dx.doi.org/10.1667/RR2892.1.S1).

Dose response and effect modification. There was a significant linear dose-response relationship ($P < 0.001$) with some indication of upward curvature ($P = 0.05$), much of which was influenced by 4 cases with unweighted shielded kerma estimates in excess of 4 Gy. After adjusting for the high-dose cases by including a dichotomous indicator, there was no evidence of significant curvature ($P = 0.13$). Figure 3b shows the estimated linear dose response. In our preferred ALL model (described below), the number of radiation-associated ALL cases was estimated to be 21.6 (Table 8). About 67% of the cases among cohort members with doses in excess of 5 mGy were associated with radiation exposure.

The ERR for ALL decreased markedly over time ($P < 0.001$). This decrease was described as proportional to attained age to the power –3.51 (Table 9). The ERR for women was about 40% of that for men. This gender- and attained-age-dependent ERR model (AIC = 496.4) described the data better than a model that included joint effects of age at exposure (higher for younger ages) and time since exposure (decreasing with time) (AIC = 502.7). As illustrated in Fig. 3c, this model predicted extremely

TABLE 6
Preferred Model, Excess Risk Parameter Estimates for Acute Myeloid Leukemia

Risk model	Quadratic dose coefficient (at 1 Gy)	Attained age		Age at exposure	
		Linear	Quadratic	Linear	Quadratic
ERR†	1.11 (0.53, 2.08)	–0.89 (–2.29, 0.41)		0.17 (–0.15, 0.50)	0.25 (0.09, 0.41)
EAR‡	1.59 (0.95, 2.41)	2.59 (0.90,4.26)	1.43 (0.44, 2.32)		

† The preferred ERR model is quadratic in dose with log-linear effect modification depending on log(attained age) and a linear-quadratic function of age at exposure. The baseline model parameters and explicit details about the dose effect modification term are given in supplementary Table S2 (http://dx.doi.org/10.1667/RR2892.1.S1). Supplementary Table S7 (http://dx.doi.org/10.1667/RR2892.1.S2) presents information on alternative ERR models. The dose coefficients describe the ERR at 1 Gy at age 70 after exposure at age 30.

‡ The preferred EAR model is quadratic in dose with log-linear effect modification depending on a linear-quadratic function of log(attained age). The baseline model parameters and explicit details about the dose effect modification term is given in supplementary Table S2 (http://dx.doi.org/10.1667/RR2892.1.S1). Supplementary Table S7 (http://dx.doi.org/10.1667/RR2892.1.S2) presents information on alternative EAR models. The dose coefficients describe the excess cases per 10,000 person years at 1 Gy at age 70.

TABLE 7
Observed and Fitted Excess Cases of Acute Myeloid Leukemia by Time Period and Age at Exposure with Category-Specific ERR Estimates

	Age at exposure									
	0–19		20–39		40+		Total			
Period	Obs	Exc†	Obs	Exc	Obs	Exc	Obs	Exc	ERR‡ (95%CI)	
1950–1955	4	3.1	3	0.7	4	2.5	11	6.4	3.6	(0.7 to 10.2)
1956–1959	7	1.3	3	0.7	8	2.2	18	4.2	9.0	(3.5 to 19.2)
1960–1969	7	2.1	7	1.7	10	3.9	24	7.7	3.1	(1.1 to 6.7)
1970–1979	7	2.3	21	2.1	13	2.4	41	6.8	1.9	(0.4 to 4.7)
1980–1989	12	3.0	20	2.2	7	1.1	39	6.3	1.8	(0.6 to 4.0)
1990–2001	19	3.9	23	1.9	1	0.3	43	6.1	1.5	(0.4 to 3.4)
Total	56	15.7	77	93	43	12.2	176	37.4		
ERR‡ (95% CI)	2.3 (1.0 to 4.5)		2.0 (0.9 to 3.8)		3.4 (1.5 to 6.6)		2.4 (1.5 to 3.7)			

† Excess cases based on preferred ERR model described in the text and Table 6 with additional details in supplementary Table S2 (http://dx.doi.org/10.1667/RR2892.1.S1).
‡ ERR at 1 Gy for a quadratic dose response model with categorical period and age-at-exposure effects.

large ERRs for those exposed as children. Virtually all of the 22 cases among those exposed before age 20 could be attributed to radiation exposure.

The radiation effect on the ALL risk could be described equally well (AIC = 496.4) using an EAR model, as illustrated in Fig. 3e. In our preferred EAR model, the excess rate decreased in proportion to age to the power −1.81 (Table 9). There was a significant gender difference ($P = 0.05$) with an estimated female:male EAR ratio of 0.40. The gender-averaged EAR at age 70 was 0.16 radiation-associated cases per 10,000 person years per Gy (95% CI 0.05– 0.38). Parameter estimates with confidence intervals for the preferred ALL ERR and EAR models are given in Table 9. The precise form of this model is given in supplementary Table S2 (http://dx.doi.org/10.1667/RR2892.1.S1) and information on the fit of alternative models is given in supplementary Table S8 (http://dx.doi.org/10.1667/RR2892.1.S2). The ALL EAR could be described almost as well using a combination of age-at-exposure and time-since-exposure effects in place of the attained age effect (supplementary Table S8; http://dx.doi.org/10.1667/RR2892.1.S2).

Both the ERR and EAR results indicated that the radiation-associated risks have decreased over time, but also suggested that dose-related increased risks may persist for many years after exposure. Using a simple ERR model in which the dose response was allowed to differ for the three periods of October 1950 through December 1952, 1953–1965 and 1966–2001, we found statistically significant dose-related increases in the risk for each period. Although the ERR decreased over time, the ERR for the last period was statistically significant and had a population average 3.1 (95% CI 0.6–10.4, $P = 0.001$) (results not shown).

Chronic Myeloid Leukemia (CML)

There were 75 eligible CML cases (63 in Hiroshima, 12 in Nagasaki) including 13 cases that occurred after 1987. The CML baseline rate increased with attained age ($P < 0.001$) with a significant difference in the age pattern for men and women ($P = 0.004$) (Fig 4a). Baseline rates for men were higher than those for women prior to age 75, but women had higher rates later in life, because the rates for women rose more rapidly than those for men. There was no indication of a birth cohort effect ($P > 0.5$). After allowing for a city difference in the dose response (described below), the baseline rates did not differ significantly by city ($P > 0.5$). The CML baseline rate model and parameter estimates are given in supplementary Table S2 (http://dx.doi.org/10.1667/RR2892.1.S1).

Dose response and effect modification. CML rates exhibited a statistically significant ($P < 0.001$) linear dose-response relationship that was not improved by the addition of a quadratic term ($P > 0.5$). The dose-response curve is shown in Fig. 4b. In our preferred ERR model for CML, the ERR was dependent on city and both time since exposure and attained age. As shown in Table 11, the estimated ERR was 5.24 per Gy standardized to attained age 55 and 25 years after exposure, and the ERR in Nagasaki was estimated to be 22% of that in Hiroshima ($P = 0.01$). There was no indication that the ERR differed by gender ($P > 0.5$).

The ERR decreased significantly in proportion to time since exposure to the power −1.59 at any attained age. The ERR decreased significantly in proportion to attained age to the power −1.42. Using the preferred ERR model the observed number of radiation-associated cases was estimated to be 33.4 with the attributable fraction among those exposed to 5 mGy or more estimated to be 64% (Table 10). Parameter estimates with confidence intervals for the preferred CML ERR and EAR models are given in Table 11, respectively. The precise form of this model is given in supplementary Table S2 (http://dx.doi.org/10.1667/RR2892.1.S1). Figure 4c and d illustrate the temporal pattern for the Hiroshima ERR for this model as a function

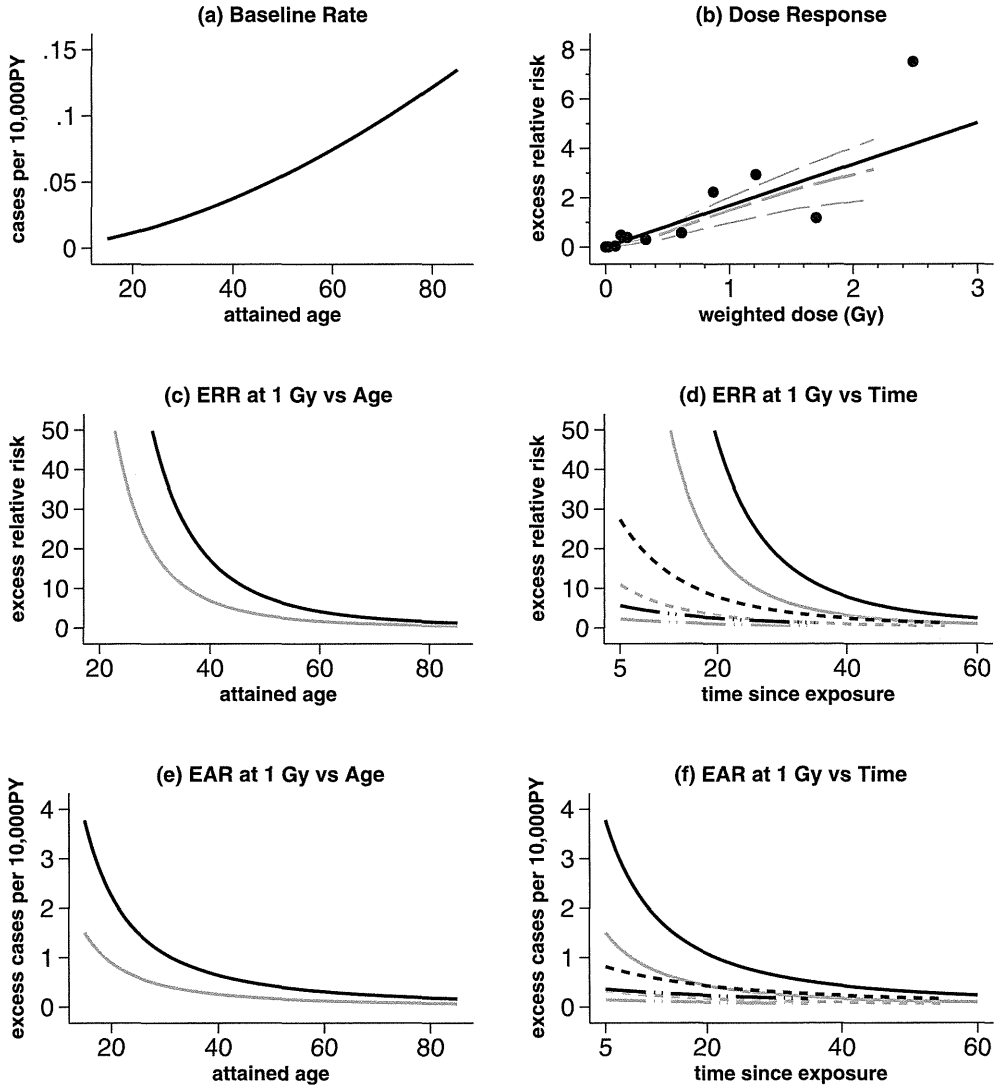

FIG. 3. LSS acute lymphoblastic leukemia risk summary plots. Panel a: shows age-specific Hiroshima baseline rate for LSS cohort members. Panel b: illustrates the radiation dose response based on the ERR model with gender average risks standardized to attained age 70. The solid-black line illustrates the fitted linear dose response. The points are based on a nonparametric dose response model, while the middle-dashed-gray line is a smoothed version of the dose category-specific estimates from the nonparametric fit. The upper- and lower-dashed-gray lines are plus and minus one standard error from the smoothed fit. Panels c and d: exhibit the temporal patterns for men (black line) and for women (gray line) in either city based on the preferred ERR model. Plots (e) and (f) present the temporal pattern for males (black) and females (gray) based on the preferred EAR model. In panels e and f: different line patterns are shown for ages at exposure of 10 (solid line), 30 (dash line) and 50 years (dash-dot line).

of attained age and time since exposure for exposure ages of 10, 30 and 50 years, respectively.

A model in which the ERR varied jointly with age at exposure, time since exposure and city (AIC = 777.7) described the data as well as the attained age, time since exposure and city model described above (AIC = 776.4). However, a model in which the ERR varied with attained age, age at exposure and city fit less well (AIC = 782.0). Parameter estimates and AIC values for these and other alternative models for the CML excess risk are given in supplementary Table S9 (http://dx.doi.org/10.1667/RR2892.1.S2).

In our preferred EAR model, the excess rate depended on city, time since exposure and a gender-dependent attained age effect. The gender-averaged EAR at age 55 after exposure at age 30 was 0.62 cases per 10,000 PY per Gy (95% CI 0.27–1.15). Excess rates for Nagasaki were about 23% of those in Hiroshima ($P = 0.01$). Figure 4e and f show the CML EAR temporal trends by gender and different age-at-exposure groups based on the preferred EAR model. For a given age at exposure, the decrease in the EAR was proportional to time since exposure to the power -1.63 ($P < 0.001$). The attained age effect differed significantly for men and women ($P = 0.01$). For any given time since exposure, the EAR for men exhibited little variation with attained age, decreasing in proportion to attained age to the power -0.20 ($P > 0.5$). Conversely, for women the EAR increased significantly ($P = 0.009$) with

TABLE 8
Observed and Fitted Background and Excess Cases of Acute Lymphoblastic Leukemia by Weighted Bone Marrow Dose Category

Dose (Gy)	Person years	Observed cases	Fitted cases†	
			Background	Excess
<0.005	2,039,093	11	12.0	0.06
–0.1	957,889	8	5.7	1.6
–0.2	201,935	4	1.2	1.6
–0.5	206,749	2	1.3	3.4
–1	117,855	5	0.7	4.0
–2	64,122	5	0.4	4.5
2+	25,761	8	0.1	6.4
Total	3,613,404	43	21.4	21.6

† Estimates based on the preferred linear ERR model described in the text and Table 9 with more details in supplementary Table S2 (http://dx.doi.org/10.1667/RR2892.1.S1).

increasing attained age. This increase was proportional to attained age to the power 2.10. The preferred EAR (AIC = 779.7) and ERR model (AIC = 776.4) described the data about equally well.

Joint Analysis of AML, ALL and CML Dose Response

The results described provide clear evidence of a time-varying radiation dose response for AML, ALL and CML. As noted in the text and illustrated in Figs. 2, 3 and 4, the temporal patterns and shapes of the dose response appear to differ for these three broad leukemia subgroups. We carried out a joint analysis using the methods described in refs. (*4*) and (*35*) to formally examine the evidence for differences in the nature of the temporal patterns and shapes of the dose response for these three subgroups.

When the subgroups are fit with group-specific baseline rates and the linear-quadratic ERR model developed for all leukemias other than CLL or ATL ("common model"), the AIC was 2,848.8. This is considerably larger than the AIC of 2,825.0 obtained using the preferred subgroup-specific models described above. For EAR models, the AIC using the common EAR model was 2,858.1, while the AIC based on the preferred subgroup-specific EAR models was 2,827.5. Although a formal test of statistical significance is not possible, based on a comparison of the differences between the AICs for the common and group-specific models, there is a clear indication of subgroup differences for both the ERR and EAR models.

In the ERR model, there is evidence of significant heterogeneity relative to the common model with regard to variation in the risk with attained age ($P = 0.01$), time since exposure ($P = 0.004$) and city ($P = 0.03$). When the effect modification was allowed to have the form of the preferred model in each subgroup, there was little evidence of significant inter-subgroup variability in the dose-response curvature ($P = 0.14$).

Test for heterogeneity in EAR effect modification relative to the common EAR model indicates some evidence of heterogeneity with regard to gender ($P = 0.04$). After allowing for gender variation, there is evidence of heterogeneity with regard to time-since-exposure ($P = 0.01$) or age-at-exposure ($P = 0.04$) effects. As with the ERR model, there was little evidence of significant inter-subgroup variability in the dose-response curvature ($P = 0.17$).

Table 12 contains estimates of the possible number of radiation-associated excess cases by time period (for all age-at-exposure groups together) based on the preferred ERR models for AML, ALL and CML. The largest number of excess cases was seen during the first 5 years of follow-up. Table 12 also provides information on the within-period distribution of the excess over the three subtypes considered here. It can be seen that, while most of the excess cases in the 1950–1955 period are CML, as time has gone on AML has come to account for most of the excess.

Chronic Lymphocytic Leukemia (CLL)

CLL is rare in Japan. In the previous report, there were only four CLL cases, which were analyzed with the other leukemias. With additional follow-up time, 12 CLL cases

TABLE 9
Preferred Model, Excess Risk Parameter Estimates for Acute Lymphoblastic Leukemia

Risk model	Linear dose coefficient (at 1 Gy)	Gender ratio (F:M)	Attained age (power)
ERR† Female	0.95 (0.23, 3.37)	0.40 (0.14, 0.99)	–3.51 (–5.29, –1.92)
Male	2.40 (0.63, 7.90)		
EAR‡ Female	0.09 (0.03, 0.25)	0.40 (0.14, 0.99)	–1.81 (–2.56, –1.08)
Male	0.23 (0.07, 0.58)		

† The preferred ERR model is linear in dose with log-linear effect modification depending on log (attained age) and gender. The baseline model parameters and explicit details about the dose effect modification term are given in Table S2 in the supplementary material (http://dx.doi.org/10.1667/RR2892.1.S1). Supplementary Table S8 (http://dx.doi.org/10.1667/RR2892.1.S2) presents information on alternative ERR models. The dose coefficients describe the ERR at 1 Gy at age 70.

‡ The preferred EAR model is linear in dose with log-linear effect modification depending on log (attained age) and gender. The baseline model parameters and explicit details about the dose effect modification term are given in Table S2 in the supplementary material (http://dx.doi.org/10.1667/RR2892.1.S21). Supplementary Table S8 (http://dx.doi.org/10.1667/RR2892.1.S2) presents information on alternative EAR models. The dose coefficients describe the excess cases per 10,000 person years at 1 Gy at age 70.

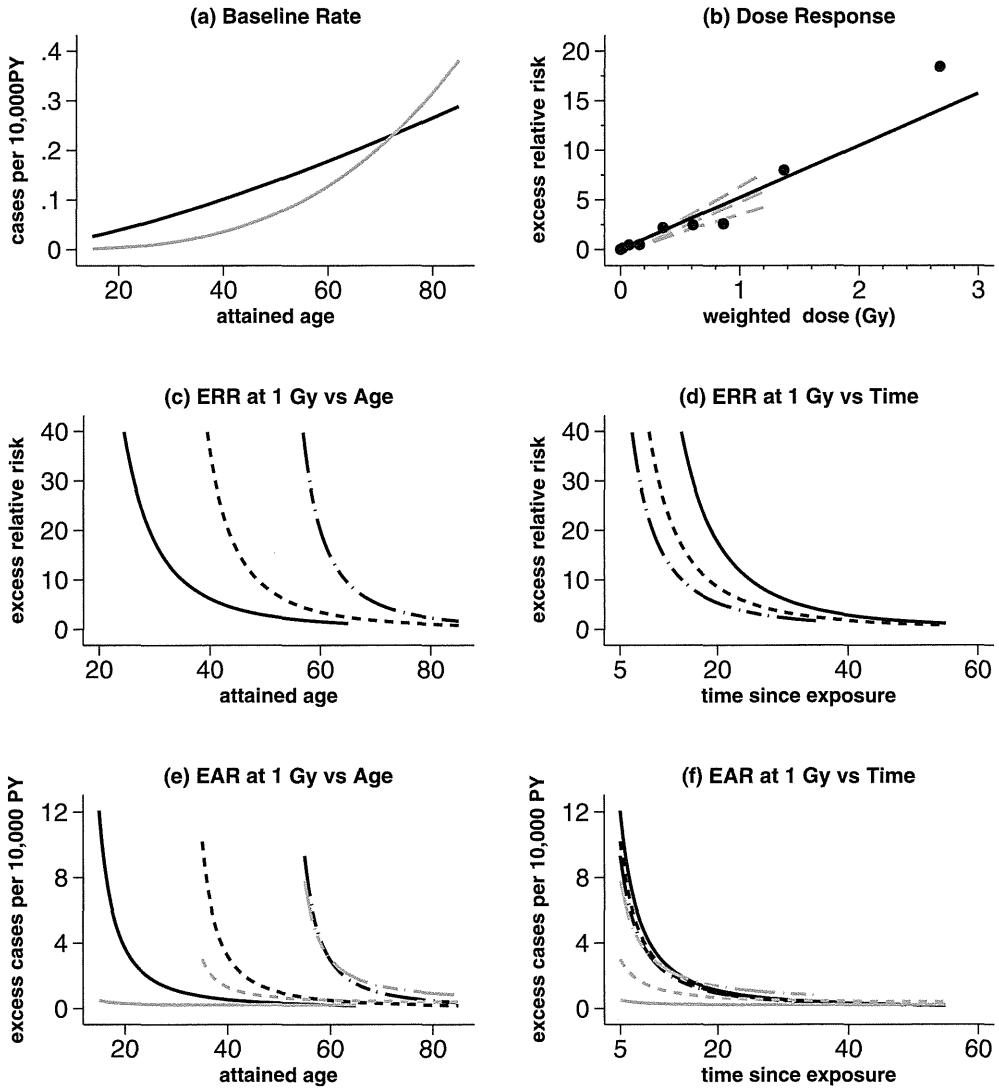

FIG. 4. LSS chronic myeloid leukemia risk summary plots. Panel a: shows age-specific Hiroshima baseline rate for LSS cohort members for men (black line) and women (gray line). Panel b: illustrates the radiation dose response based on the ERR model with gender average risks standardized to time since exposure at 25 and at attained age 55. The solid-black lines illustrates the fitted linear dose response. The points are based on a nonparametric dose response model, while the middle-dashed-gray line is a smoothed version of the dose category-specific estimates from the nonparametric fit. The upper- and lower-dashed-gray lines are plus and minus one standard error from the smoothed fit. Panels c and d: illustrate the temporal pattern and age-at-exposure effects for our preferred ERR model. Curves are shown for ages at exposure 10 (solid curve), 30 (dash line) and 50 years (dash-dot line) in Hiroshima. The ERR does not depend on gender. Panels e and f: present the temporal pattern and age-at exposure effects by gender based on the preferred EAR model in Hiroshima. Curves are shown for age at exposure 10 (solid line), 30 (dash line) and 50 years (dash-dot line) with black and gray lines for men and for women, respectively.

were identified including 10 cases classified as chronic lymphocytic leukemia and 2 as hairy cell leukemia. The newly identified cases included only one case among the not-in-city cohort members and 7 cases diagnosed after 1987. Using a simple age- and gender-adjusted baseline model, a significant linear dose response was detected, which suggested that CLL risk might be increased at higher doses ($P < 0.05$).

Adult T-Cell Leukemia (ATL), Nagasaki Only

There were a total of 47 eligible ATL cases. Due to the fact that there were only 5 ATL cases in Hiroshima, the analyses were limited to Nagasaki. The background rate exhibited a rapid increase with attained age that was proportional to the power 4.07 (95% CI 2.59–5.74, $P < 0.001$). Age-specific ATL rates in Nagasaki have changed significantly over time ($P = 0.01$), with rates estimated to have increased by about 34% for each decade increase in the year of birth (95% CI 7–71%). There were no statistically significant gender differences in the ATL baseline rates ($P > 0.5$). Figure 5 shows the increasing rates of ATL by age. The ATL baseline rate model and parameter estimates are given in supplementary Table S2 (http://dx.doi.org/10.1667/RR2892.1.S1).

TABLE 10
Observed and Fitted Background and Excess Cases of Chronic Myeloid Leukemia by Weighted Bone Marrow Dose Category

Dose (Gy)	Person years	Observed cases	Fitted cases†	
			Background	Excess
< 0.005	2,039,093	22	22.5	0.1
0.1	957,889	17	11.6	2.9
0.2	201,935	2	2.5	3.0
0.5	206,749	11	2.6	6.5
1	117,855	6	1.4	7.5
2	64,122	9	0.7	7.5
2+	25,761	8	0.3	5.9
Total	3,613,404	75	41.6	33.4

† Estimates based on the preferred linear ERR model described in the text and Table 11 with more details in supplementary Table S2 (http://dx.doi.org/10.1667/RR2892.1.S1).

Dose response and effect modification. There was no evidence of a dose response for ATL ($P > 0.5$) and the ERR/Gy in a linear model was estimated as 0.05 (95% CI −0.51–1.54). Because of a lack of cases among women who received high doses, the ERR/Gy for women was estimated to be les than zero. After restricting the excess risk for women to be zero, the fit of the model was improved and the ERR/Gy estimate for men was 0.88 (95% CI −0.60–4.52, $P = 0.28$), which was not statistically significant.

Lymphoma

The 437 eligible lymphoma cases include 402 NHL and 35 HL cases with 143 of these cases diagnosed since 1987 among cohort members who were in the cities at the time of the bombings. Another 102 cases were among cohort members who were not in the cities at the time of bombings. NHL and HL risks were analyzed separately.

Non-Hodgkin lymphoma (NHL). Background rates for NHL increased rapidly with attained age. While this increase was roughly proportional to attained age to the fourth power, the fit was significantly improved when the nature of the increase was allowed to vary with increasing age, with knots at age 40 and 70 ($P = 0.007$, with 3 *df*). Age-specific rates for women were 58% of those for men (95% CI 48–72%, $P < 0.001$) with no significant ($P > 0.5$) gender difference in the nature of the increase with attained age. NHL baseline rates also exhibited a complex nonlinear birth cohort effect ($P < 0.001$) with the highest age-specific rates for cohort members born around 1940 and lower age-specific rates for people born in earlier or later years. As shown in Fig. 6a, the age-specific baseline rates for the 1935 birth cohort were at least twice those for the 1895 birth cohort. This pattern was similar to that seen for the LSS leukemia baseline rates and for Japanese national NHL rates (*33*). There was no indication of a city difference in the baseline rates ($P > 0.5$). The NHL baseline rate model and parameter estimates are given in supplementary Table S2 (http://dx.doi.org/10.1667/RR2892.1.S1).

Dose response and effect modification. There was no evidence of a significant dose response in the ERR ($P = 0.23$) in a simple linear dose-response model. However, when the ERR was allowed to differ for men and women, there was a suggestion of an elevated risk in men (ERR/Gy = 0.46; 95% CI −0.08 to 1.29, $P = 0.11$), but no indication of an effect for women (ERR/Gy = 0.02; 95% CI <−0.44 to 0.64, $P > 0.5$). Allowing the ERR for men to vary with attained age led to a significant improvement in the fit relative to a model with no radiation effects ($P = 0.005$, with 2 *df*). Thus, while there was some evidence of a statistically

TABLE 11
Preferred Model, Excess Risk Parameter Estimates for Chronic Myeloid Leukemia

Risk model		Linear dose coefficient (at 1 Gy)	City ratio (N:H)	Gender ratio (F:M)	Attained age (power)	Time since exposure (power)
ERR†	Hiroshima	5.24 (1.92, 11.8)	0.22 (0.03, 0.75)		−1.42 (−3.04, 0.01)	−1.59 (−2.34, −0.95)
	Nagasaki	1.17 (−0.10, 4.71)				
EAR‡	Female					
	Hiroshima	0.57 (0.23, 1.10)	0.23 (0.03, 0.76)	0.84 (0.34, 2.21)	2.10 (0.48, 4.21)	−1.63 (−2.38, −0.97)
	Nagasaki	0.13 (<0, 0.47)				
	Male					
	Hiroshima	0.68 (0.24, 1.49)			−0.20 (−1.03, 0.66)	
	Nagasaki	0.15 (<0, 0.60)				

† The preferred ERR model is linear in dose with log-linear effect modification depending on log (attained age), log (time since exposure) and city. The baseline model parameters and explicit details about the dose effect modification term are given in Table S2 in the supplementary material (http://dx.doi.org/10.1667/RR2892.1.S21). Supplementary Table S9 (http://dx.doi.org/10.1667/RR2892.1.S2) presents information on alternative ERR models. The dose coefficients describe the ERR at 1 Gy at age 55 after exposure at age 30.

‡ The preferred EAR model is linear in dose with log-linear effect modification depending on city, sex, log(time since exposure) and log(attained age) with the attained age effect differing in the two cities. The baseline model parameters and explicit details about the dose effect modification term is given in Table S2 in the supplementary material (http://dx.doi.org/10.1667/RR2892.1.S1). Supplementary Table S9 (http://dx.doi.org/10.1667/RR2892.1.S2) presents information on alternative EAR models. The dose coefficients describe the excess cases per 10,000 person years at 1 Gy at age 55 after exposure at age 30.

TABLE 12
Radiation-Associated Excess Leukemia Cases by Subtype and Period

	Leukemia subtype†						
	AML		ALL		CML		
Period	Excess‡	Percent§	Excess	Percent	Excess	Percent	Total
1950–1955	6.3	20%	8.3	27%	16.3	53%	30.9
1956–1960	4.3	29%	4.1	28%	6.2	43%	14.6
1961–1970	7.6	43%	4.5	25%	5.7	32%	17.8
1971–1980	6.8	57%	2.4	20%	2.7	23%	11.9
1981–1990	6.2	68%	1.4	15%	1.5	17%	9.1
1991–2001	6.1	78%	0.8	10%	0.9	12%	7.8
Total	37.3	41%	21.5	23%	33.3	36%	92.1

† The subtypes considered here are acute myeloid leukemia (AML), acute lymphoblastic leukemia (ALL), and chronic myeloid leukemia (CML).

‡ Radiation-associated excess case estimates based on the preferred ERR models described in the text and in Tables 6, 9 and 11 with additional details given in supplementary Table S2 (http://dx.doi.org/10.1667/RR2892.1.S1).

§ Percentage of radiation associated excess cases within the time period.

significant radiation effect in men, there was no indication of a radiation effect in women.

As indicated by the dose-response curves in Fig. 6c, the ERR/Gy for men (dark solid curve) was large at younger ages, but declined dramatically and approached 0 by age 40. It is difficult to interpret the large ERRs for the very young since baseline rates are highly variable and imprecise due to the small number of children and young adults at risk for developing NHL. The EAR model provided a more simple and perhaps more useful description for small excess risks when baseline rates are low. There was a suggestion of a dose response ($P = 0.10$) in a simple constant EAR model. Letting the EAR depend on gender led to a significant improvement in the fit ($P = 0.048$). The estimated EAR for men was 0.54 (95% CI 0.09–1.32, $P = 0.003$) while that for women was essentially 0 (95% CI −0.02–0.31, $P > 0.5$). There was no indication that the EAR varied with attained age ($P = 0.3$), time since exposure ($P = 0.46$), or age at exposure ($P = 0.15$). Supplementary Table S2 (http://dx.doi.org/10.1667/RR2892.1.S21) contains information on the form of the final model than the parameter estimates for this model.

Figure 6d presents the fitted constant EAR for men (dark solid line) and the EAR estimate derived from the age-dependent ERR model (lighter dashed line) described above. While the EAR model suggested a persistent increase in risk, the ERR model suggested that the excess rate peaked around age 20 and that there was little excess after age 30, which also implies that the radiation effects were seen primarily among those exposed as children or young adults. Despite striking differences in the pattern of the excess risk, the goodness of fit of the ERR (AIC = 2,374.8) and EAR (AIC = 2,378.8) models was comparable. Based on the time-constant EAR model, the estimated number of radiation-associated cases over the follow-up period was estimated to be 7.8 for men and 0 for women (Table 13), with about 10% of the cases among men with doses in excess of 5 mGy attributable to the radiation exposure. The time-dependent ERR model predicts about half the number of excess cases as does the EAR model.

Hodgkin Lymphoma (HL)

There were only 35 eligible HL cases in the cohort. Age- and birth-cohort adjusted baseline rates in women were about 40% of those in men (95% CI 21–82%, $P = 0.01$). Baseline rates tended to increase with increasing attained age, but the increase was not statistically significant ($P = 0.35$). However, age-specific rates in later birth cohorts were significantly lower than those for earlier birth cohorts ($P = 0.003$). There was no indication of a city difference in the baseline rates ($P = 0.16$). HL baseline rates are plotted in Fig. 7. The HL baseline rate model and parameter estimates are described in supplementary Table S2 (http://dx.doi.org/10.1667/RR2892.1.S1).

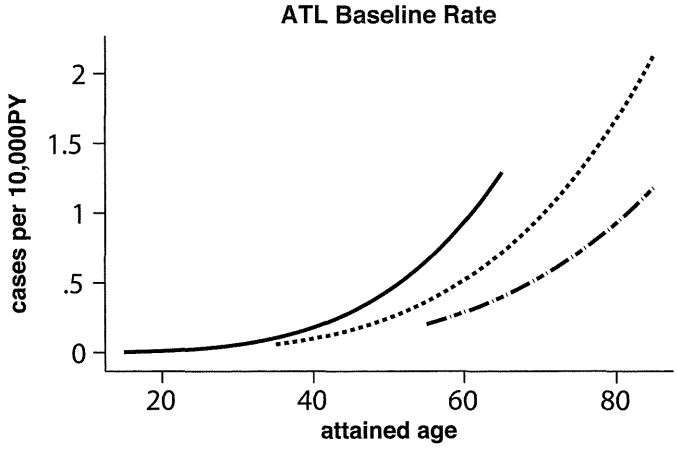

FIG. 5. LSS adult T-cell leukemia risk summary plots. The plot shows age-specific Nagasaki baseline rates (zero dose) for LSS cohort members born in 1895 (dash-dot line), 1915 (dash line) and 1935 (solid line). There is no significant dose response.

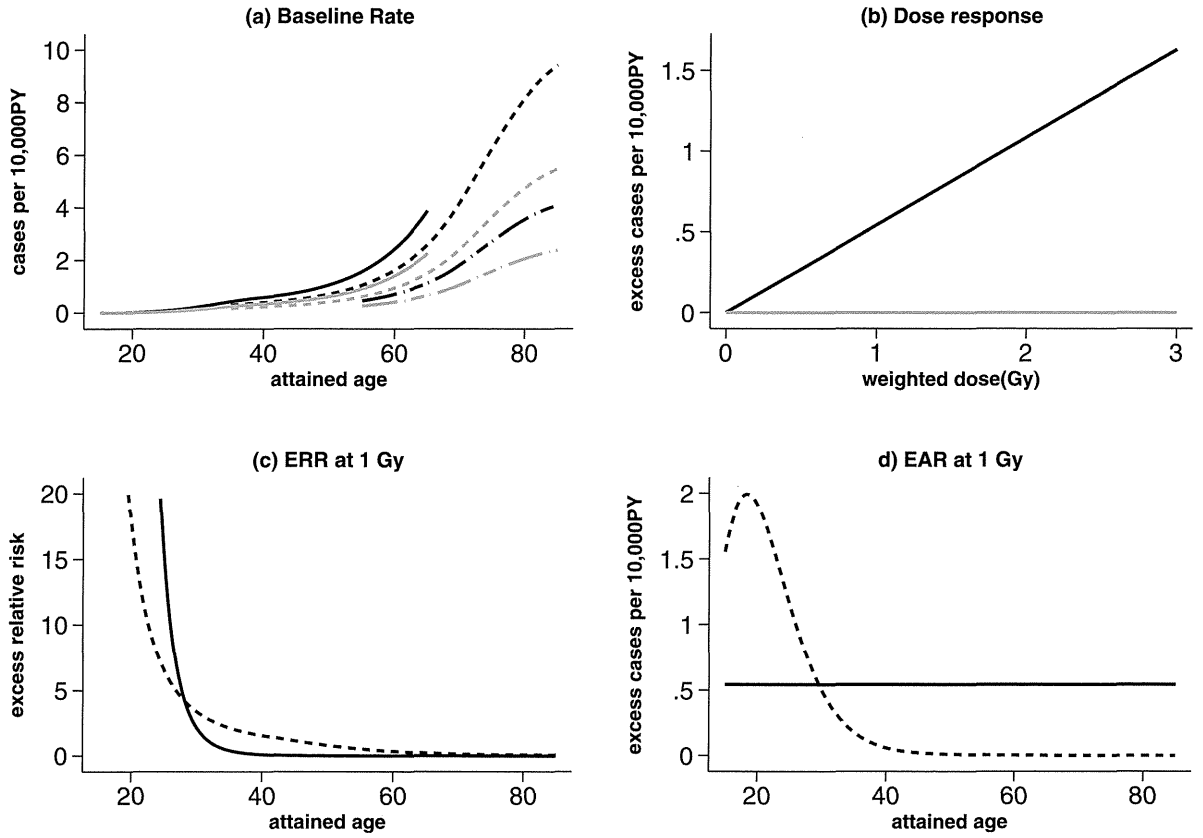

FIG. 6. LSS non-Hodgkin lymphoma risk summary plots. Panel a: shows age-specific Hiroshima baseline rates for LSS cohort members. Curves are shown for birth cohorts 1895 (dash-dot line), 1915 (dash line) and 1935 (solid line) model with black and gray lines for men and for women, respectively. Panel b: illustrates the radiation dose response based on the EAR model with black and gray lines for men and for women, respectively. Panel c illustrates the ERR temporal pattern for men. The solid line shows the predicted ERR based on our preferred ERR model, and the dotted line is the ERR derived from our preferred EAR model. Panel d: presents the EAR temporal pattern for men. The dotted line shows the predicted EAR based on our preferred EAR model and the solid curve is the EAR derived from our preferred ERR model.

Dose response and effect modification. No significant dose response was found for HL (ERR/Gy = 0.20; 95% CI −1.03–2.63, $P > 0.5$). Allowing the dose response to depend on gender did not improve the fit of the model ($P > 0.5$), nor was there any indication of statistically significant variation in the ERR with age ($P > 0.5$). The estimated time constant EAR was essentially 0 ($P > 0.5$).

Multiple Myeloma (MM)

Among the 181 cases of MM identified in this study, 136 were eligible for use in the risk analyses including 36 cases diagnosed in survivors after 1987 and 31 cases diagnosed among cohort members who were not in the cities at the time of the bombings.

Baseline rates varied significantly with both attained age ($P < 0.001$) and birth cohort ($P < 0.001$). The birth cohort effect appeared to be non-monotonic, with the largest age-specific rates seen for people born around 1920 and decreasing by about 35% per decade for earlier and later birth cohorts. This pattern was generally similar to that seen in leukemia other than CLL or ATL in this cohort. The increase in rates was roughly proportional to attained age to the power 5.45 (95% CI 4.41–6.55, $P < 0.001$). However, the model was significantly improved ($P = 0.01$) when the baseline rate was allowed to increase to about age 80 and level out, or even decrease later in life (Fig. 8).

TABLE 13
Observed and Fitted Background and Excess Cases of Non-Hodgkin Lymphoma Cases by Weighted Bone Marrow Dose Category

Dose (Gy)	Person years	Observed cases	Fitted cases†	
			Background	Excess
<0.005	2,039,093	226	221.6	0.02
–0.1	957,889	99	104.2	0.6
–0.2	201,935	21	22.7	0.6
–0.5	206,749	28	22.9	1.3
–1	117,855	13	13.2	1.7
–2	64,122	14	7.1	2.0
2+	25,761	1	2.5	1.6
Total	3,613,404	402	394.2	7.8

† Estimates based on the preferred linear EAR model described in the text with additional details in supplementary Table S2 (http://dx.doi.org/10.1667/RR2892.1.S1). This is gender-dependent, time-constant linear EAR model with an EAR of 0.54 cases per 10,000 PY at 1 Gy and no excess risk for women.

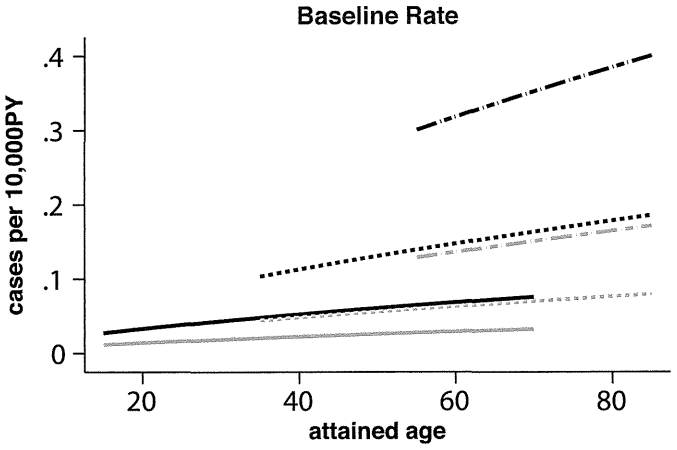

FIG. 7. LSS Hodgkin lymphoma. The plot shows age-specific baseline rates (zero dose) for LSS cohort members born in 1895 (dash-dot line), 1915 (dot line) and 1935 (solid line). The black lines are for men and the gray lines are for women. There is no significant dose response.

The background risk did not vary significantly with either gender ($P = 0.16$) or city ($P = 0.12$). Supplementary Table S2 (http://dx.doi.org/10.1667/RR2892.1.S1) contains information on the form of the final baseline rate model with the associated parameter estimates.

Dose response and effect modification. The ERR/Gy estimate of 0.38 from a linear dose-response model was not statistically significant (95% CI −0.23–1.36, $P = 0.21$) The fit was not improved by the addition of a quadratic term ($P = 0.44$). There was no evidence of statistically significant variation in the ERR with gender ($P > 0.5$), attained age ($P = 0.31$) or age at exposure ($P > 0.5$).

When the data were described using a constant linear EAR model, the estimated EAR was 0.07 cases per 10,000 PY per Gy (95% CI <–0.05–0.29, $P = 0.25$), with no indication of variation with gender ($P = 0.5$), attained age ($P = 0.33$) or time since exposure ($P > 0.5$). This point estimate of the EAR is almost identical to that reported 15 years ago. As in the previous report, we conclude that there is no evidence of a statistically significant radiation-associated excess risk of incident MM in the atomic bomb survivors.

DISCUSSION

Our study extends the follow-up 14 years beyond that used in the last major report on hematological malignancies in the LSS cohort (*4*), providing incidence follow-up for 55 years. This has been made possible because of the active ascertainment and review of hematopoietic malignancies already in place when the cohort was established in late 1950, together with the subsequently established tumor registries in Hiroshima and Nagasaki. Due to incomplete ascertainment of incident cases among cohort members who moved away from Hiroshima or Nagasaki, a probabilistic adjustment for migration was included in the analyses as with all other major LSS incidence reports. Diagnostic criteria and type definitions for hematopoietic malignancies have evolved and been refined over time, but the reclassification of leukemia types for cases diagnosed before the mid-1980s using the recent classifications has enabled us to use diagnostic categories that are consistent with and generally as detailed as those used in other studies of radiation effects on these malignancies.

In contrast to the earlier report (*4*) that focused exclusively on time-since-exposure dependent EAR models with, in most cases, categorical age-at-exposure effects, we assessed excess risk in this report using ERR and EAR models with simple continuous functions of age at exposure and either attained age or time since exposure. We found that those smooth models describe the data as well as the partially categorical models used in ref. (*4*). We also found that while both ERRs and EARs for leukemia other than CLL or ATL as a group have declined over the follow-up period for all ages at exposure (Fig. 1d and f), the excess risks do not appear to have fallen to zero by the end of the follow-up—55 years after exposure. The temporal variation of either the ERR or EAR as described in terms of (post-

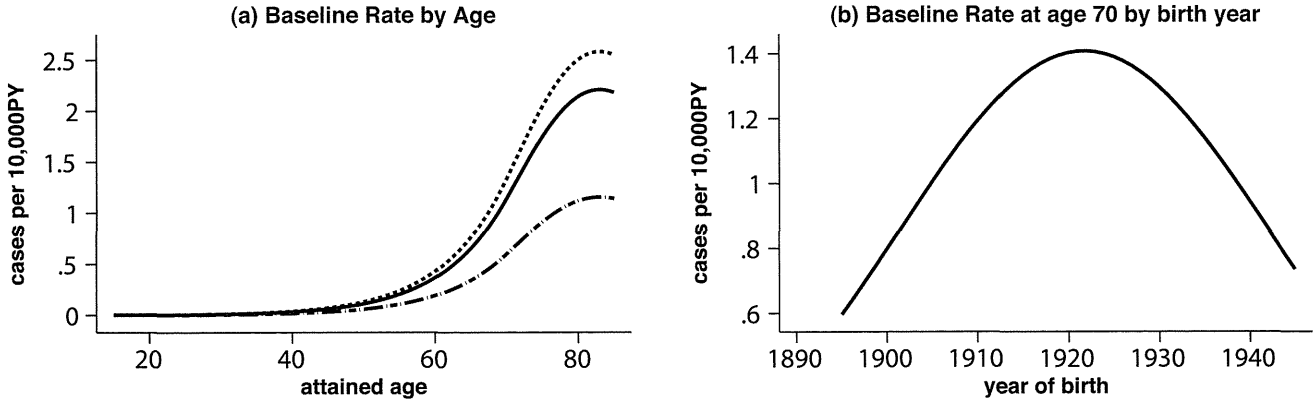

FIG. 8. LSS multiple myeloma summary plots. Panel a: shows age-specific baseline rate (zero dose) for LSS cohort members born in 1895 (dash-dot line), 1915 (dash line) and 1935 (solid line). Panel b: shows the baseline rate by birth year at attained age 70.

TABLE 14
Comparison of Risk Estimates to Selected Cohort Studies

Study cohort	Cancer end point	Follow-up	Cases	Average dose (range)	Dose response model	ERR: Leukemia excluding CLL (95% CI)
3rd NRRW	incidence	1955–2001	234	0.025 Sv (>0, 0.1+)	Linear	1.78 (0.17, 4.36)
A-bomb LSS cohort† (males, 20<=age at exposure <60)	incidence	1950–2001	93	0.50 Gy (0, 3.16)	Linear	2.04 (0.33, 6.85)
Techa River cohort	incidence	1953–2005	70	0.3 Gy (0, 2.0)	Linear	4.9 (1.6, 14.3)
A-bomb LSS cohort‡	incidence	1950–2001	312	0.64 Gy (0, 4.54)	Linear	2.78 (1.84, 4.01)

† The analysis is restricted to men who were exposed to A-bomb radiation at age 20–60 with weighted bone marrow dose $\leq$4 Gy. The ERR coefficient describes the excess RR at 1 Gy at age 50 after exposure at age 25.

‡ This analysis is for the full LSS cohort excluding unknown dose. The ERR coefficient describes the excess RR at 1 Gy at age 60 after exposure at age 25.

exposure) attained age highlights that, while highest excess risks are seen shortly after exposure for those exposed as children, at any given attained age the excess risks are generally higher for those exposed later in life (Fig. 1c and e). In addition, the NIC group was used in this study to augment the information on the variation in baseline rates. When all leukemias (or subtypes) other than CLL/ATL were examined, the inclusion or exclusion of the NIC group did not substantially change the risk estimates.

Richardson *et al.* (*7*) recently considered an ERR model for the LSS leukemia mortality in which the temporal variation was described in terms of an age-at-exposure dependent log cubic spline in time since exposure. That model (AIC = 2,445.6) did not describe the leukemia incidence data as well as did our preferred ERR model (AIC = 2,431.9).

In the BEIR VII study (*36*) and some other recent work on the LSS leukemia mortality data (*7*), the age-at-exposure effect on the excess risks was not allowed to vary among people who were more than 30 years old at the time of exposure. Imposing this constraint on our models resulted in a markedly poorer fit (AIC = 2,438.4 for the constrained model versus 2,431.89 for our preferred leukemia other than CLL or ATL model).

A major focus of this report was on the leukemia other than CLL or ATL as a group, which includes data on several different types of leukemia. To the extent that the cell-type distribution of the cases in this group in the LSS resembles that of many non-Japanese populations, the LSS risk data for this group can be useful for prediction or comparison with the radiation-related risk of leukemia other than CLL in other irradiated populations. Carrying out such additional analyses, we found that the predicted ERRs in the LSS cohort are consistent and comparable to those estimated in the studies of the National Registry of Radiation Workers (*37*) and the Techa River Cohort (*38*). Table 14 gives the comparison of risk estimate of the LSS cohort based on a relevant subset to the aforementioned cohorts.

Another focus was to characterize the radiation-related risk for specific types of leukemia. Leukemias other than CLL or ATL as a group, as well as ERRs for AML, ALL and CML considered separately, declined over time for all age groups. The temporal patterns in the type-specific EAR estimates are more complicated. Our analyses suggested that AML excess rates may have increased slightly over time, especially among people exposed after about age 30, while the EARs for ALL and CML have decreased over time. Those declines have often been interpreted as suggesting that the leukemia excess rates among the exposed returned to baseline levels 10–20 years after exposure. However, the analyses in this paper indicated that this is not the case for AML and ALL, as there was evidence of persistent risks 30 to 50 years after exposure for each of these types.

Cell-type specific leukemia risks and especially how they are modified by age and time, may be more useful in considering possible biological mechanisms for radiation-associated leukemogenesis than from analyses of a heterogeneous group of several types of leukemia combined. Some striking contrasts were noted between the type-specific excess rates. First, while AML exhibited a nonlinear upward-curving dose response, there was no evidence against linearity for either ALL or CML. Also, as noted above, AML excess rates tended to increase with increasing attained age for those exposed as adults, while ALL and CML excess rates appeared to decrease over time. While the radiation-related risk of CML seemed to decline with both age at exposure and time since exposure, the ALL excess rates decreased with attained age, but did not vary with either age at exposure or time since exposure.

The data suggest that the radiation associated excess rates for AML follow a U-shaped pattern in age, with excess rates falling for the youngest cohort members (who had to have been exposed early in life) and then increasing with attained age regardless of age at exposure. Although the current preferred EAR model for AML is much more simple than the 1994 model that involved complex interactions between age at exposure and time since exposure, the variation in the fitted excess rates with age are quite similar as shown in Fig. 2e and f. The temporal patterns for the ALL and CML excess rates differ significantly from those seen for AML. In

particular, excess rates for both ALL and CML, which were considerably greater than those for AML in the period shortly after the bombings, have decreased markedly over time. Thus, as indicated in Table 12, ALL and CML cases were the most common radiation-associated types and account for about 75% of the excess cases during the first 5 years of follow-up, i.e., years 5–10 after radiation exposure. If radiation markedly increased leukemia risks prior to 1950, as seems especially likely for ALL and CML, then the proportion of the radiation-associated excess ALL and CML cases in the first decade after exposure is likely to be even more striking than that which was suggested by the available data.

As the cohort members have aged, AML has become the predominant radiation-associated leukemia, accounting for over 80% of excess leukemia cases during the last 15 years of follow-up. It has been suspected that leukemia may be induced by specific translocations caused by radiation. However, spontaneous translocations specific to ALL are much more frequent than AML cases bearing the translocations. In addition, radiation-induced DNA damage is essentially random in the genome. Based on these observations, Nakamura (*39*) recently speculated that the radiation-related ALL risk in a population is almost entirely attributable to a small number of predisposed individuals in whom translocation-carrying pre-ALL cells have accumulated. He suggested that the short latency period for radiation-related ALL risk at young ages may be due to the small number of events needed for the conversion of pre-ALL cells present in newborns to full malignancy. Although CML occurs primarily in the elderly, the temporal risk pattern for CML is similar to that of ALL. BCR/ABL fusions have been linked to the majority of CML cases, but are also common in the general population (*40*). It may be that a very few additional mutations are required to convert the translocation-bearing pre-leukemic cells to tumor cells. Nakamura suspected the possibility of two different mechanisms: one for young-onset AML, which is clonally expanded similar to ALL, and the other for non-translocation-type AML, which like solid cancers, predominates in middle- and older-aged individuals, requiring a multi-step leukemogenesis process. The temporal patterns that we find for these three leukemia subtypes are generally consistent with Nakamura's hypothesis.

A recent study of myelodysplastic syndrome (MDS) risks among Nagasaki survivors for the period from 1985–2004 (*41*) showed a significant excess risk of MDS with an ERR/Gy estimate of 4.3 (95% CI 1.6–9.5), which is about twice the AML ERR estimate for the post-1986 period. People with MDS are known to have a higher risk of developing AML. However, it is of interest to note that the ERR for MDS after 1985 is larger than that for AML and that the shape of the dose response is quadratic for AML, but approximately linear for MDS. Further data on MDS incidence among LSS Nagasaki survivors and among Hiroshima survivors would help to better understand the relationship between MDS and AML excess risks.

It is likely that some cases identified as AML in the early years would have been classified as MDS if they were diagnosed with modern criteria. However, we feel that such misclassification is unlikely to have much impact on the inferences about AML risk estimates in the LSS, since (1) AML cases prior to the mid-1980s identified as MDS in the FAB review (*18*) were not used in the current analyses, (2) misclassification is less likely in the more recent years since MDS was recognized as a distinct condition, and (3) the AML baseline risk model includes a birth cohort effect that reduces the impact of period-specific misclassification. Any misdiagnosis of MDS as AML cases is likely to be independent of dose in which case it would not affect the ERR estimate of AML risk, though it would tend to increase the EAR estimate.

Chronic lymphocytic leukemia is very rare in Japan. Due to the small number of CLL cases in the LSS, radiation effects on CLL have not been considered in previous LSS reports. Although there were only 12 eligible cases, four of which occurred among survivors with doses in excess of 0.2 Gy, a simple trend test suggested a statistically significant dose response. Our results are consistent with findings of some, though not all, studies in the literature. A recent case-control study of leukemia in Chernobyl clean-up workers in Ukraine (*29*) and another such study in Belarus, Russia and Baltic countries (*42*) have shown increased risk of both CLL and leukemia other than CLL associated with radiation exposure. Similarly, a significantly increased risk of CLL as well as non-CLL leukemia was associated with radon and/or gamma radiation exposures in uranium miners (*28*). Conversely, no evidence of radiation-associated increases in the risk of CLL were seen in various other studies including the 15-country nuclear worker study (*43*), the Techa River cohort (*38*), the Mayak worker cohort (*44*), or UK radiation workers (*37*). The suggestion of a radiation effect on CLL risks in the LSS should be interpreted with caution and generalization to other populations may be unwarranted. In most Western populations, CLL accounts for 20% or more of all leukemia cases and an even higher proportion of leukemias seen late in life, but accounts for only about 3% of the LSS cases. Clinical data suggest that Japanese CLLs are largely dormant and genetically and biologically different from nonsmoldering CLLs seen in Western populations.

The large proportion of ATL in Nagasaki is not surprising. As reported in a nationwide study on ATL in Japan, ATL is endemic in Nagasaki (*45*). In the Nagasaki LSS, 42 out of 66 leukemia incident cases (63.6%) were diagnosed with ATL. There is no evidence of a radiation effect for ATL among Nagasaki LSS subjects, which may be due to the unusually high HTLV-I infections in the region.

The evidence for radiation effects on the risks of the other types of hematopoietic malignancies considered was less

clear cut. While there is no evidence of a radiation effect or dose response for HL or MM, the finding of a significant radiation-associated increase in NHL risks for men with no evidence of a radiation effect for women is similar to what has been reported in earlier analyses of NHL incidence (*4*) and mortality in the LSS (*46*). In the recent mortality analysis, Richardson *et al.* (*46*) considered ERR models for NHL mortality among LSS men who were 15–64 years old at the time of exposure and found a significant association that was most prominent 35 or more years after exposure. This is quite different than what is seen for the incidence data in which the ERR declines markedly with age (and hence time since exposure) whether or not the analysis is restricted to working age males. In our view, at best the LSS incidence data provide rather weak support for an NHL dose response among men with no evidence to support the idea that the risks are increasing with attained age or time since exposure.

Some early reports on myeloma mortality and incidence in the LSS have shown a statistically significant dose response for MM. The reasons for the differences between the findings of the incidence analyses and these earlier analyses were discussed in (*4*). To understand the difference, we also carried out an analysis of MM mortality in the cohort used for the current study. There were 111 MM deaths during the follow-up period including 86 MM cases used in the incidence analyses, and another 19 cases that were not used in the incidence analyses because they were either second primaries (10 cases) or not resident in the catchment area at the time of diagnosis (9 cases). Four of the remaining 6 cases had been rejected by the registries, while the other 2 cases had reports of solid cancers (both reported as renal cell carcinoma) with no indication of MM or any other hematopoietic malignancies. There was no evidence of statistically significant increases in either the ERR ($P = 0.12$) or the EAR ($P = 0.3$) with dose. The ERR and EAR point estimates were similar to those given above for the incidence data. This difference is largely due to uncertainties about the diagnosis of a small number of high-dose cases for which MM reported as the cause of death was not confirmed by the in-depth hematological review conducted for the incidence study. Taken together, the data provide little, if any, evidence of a radiation effect on MM. Although some worker studies including the most recent analysis of UK National Registry for Radiation Workers (*37*) and a study based on records from the National Dose Registry of Canada (*47*) provide some suggestion of a dose response for MM, the dose-response trends seen in those studies were not statistically significant. Results for MM mortality using extended follow-up are discussed in the latest LSS mortality report (*48*).

Increases in leukemia risks were one of the earliest significant long-term health effects detected among the atomic bomb survivors. However, in view of the declining radiation-related risk over the years, it has been thought that the radiation-associated excess risks would disappear over time. The present analyses that included information on cases diagnosed 43–56 years after exposure have provided important new insights into the persistent nature of the leukemia risks. The data suggest that, while radiation-associated excess risks for ALL and CML among the exposed have essentially returned to baseline levels by the end of follow-up, AML risks have persisted with excess rates that appear to be increasing with attained age (albeit not as rapidly as the baseline rates). It seems likely that the excess AML risks will persist throughout lifetime for people exposed at any age. This is similar to the temporal pattern for solid cancers. Since 40% of the cohort including most of those exposed as children, were still alive at the end of follow-up in this study, with continued follow-up of the LSS and evolving analytical methods, we expect that further insights will be gained into radiation effects on the leukemia and other hematopoietic malignancies.

APPENDIX

The online appendix tables include a listing of the morphological codes for the subtype groups and detailed descriptions of the parameterizations and parameter estimates for the preferred baseline and excess rate (ERR and EAR) models along with tables that describe (1) the impact of migration adjustment on person years (by city, gender, birth cohort and time period), (2) crude rates (by birth cohort, time period and dose category) and (3) alternative models for leukemia other than CLL or ATL, AML, ALL and CML (http://dx.doi.org/10.1667/RR2892.1.S3).

ACKNOWLEDGMENTS

The Radiation Effects Research Foundation is a private, non-profit foundation funded by the Japanese Ministry of Health, Labour and Welfare and the U.S. Department of Energy, the latter in part through DOE award DE-HS0000031 to the National Academy of Sciences, which supported WLH, HMC and RES. This research was also supported by the U.S. National Cancer Institute contract N02-CP-2009-00005 and in part by the Intramural Research Program of the NIH Division of Cancer Epidemiology and Genetics. The views of the authors do not necessarily reflect those of the two governments. We are especially grateful to the diligent work of tracing and abstracting hospital records by the staff of the Hiroshima and Nagasaki tumor registries and of the hematologists and others who were engaged in the operation of the Leukemia Registry.

Received: December 7, 2011; accepted: November 19, 2012; published online: February 11, 2013

REFERENCES

1. Dunlap CE. Effects of radiation on normal cells. III. Effects of radiation on the blood and the hematopoietic tissues, including the spleen, the thymus, and the lymph nodes. Arch Path 1942; 3:562–608.
2. Henshaw PS, Hawkins JW. Incidence of leukemia in physicians. J Natl Cancer Inst 1944; 4:339–6.
3. Folley JH, Borges W, Yamasaki T. Incidence of leukemia in survivors of the atomic bomb in Hiroshima and Nagasaki, Japan. Am J Med 1952; 13:311–21.
4. Preston DL, Kusumi S, Tomonaga M, Izumi S, Ron E, Kuramoto A, et al. Cancer incidence in atomic bomb survivors. Part III. Leukemia, lymphoma and multiple myeloma, 1950≠1987. Radiat Res 1994; 137(2 Suppl):S68–97.
5. Pierce DA, Shimizu Y, Preston DL, Vaeth M, Mabuchi K. Studies

of the mortality of atomic bomb survivors. Report 12, Part I. Cancer: 1950–1990. Radiat Res 1996; 146(1):1–27.

6. Preston DL, Pierce DA, Shimizu Y, Cullings HM, Fujita S, Funamoto S, et al. Effect of recent changes in atomic bomb survivor dosimetry on cancer mortality risk estimates. Radiat Res 2004; 162(4):377–89.
7. Richardson D, Sugiyama H, Nishi N, Sakata R, Shimizu Y, Grant EJ, et al. Ionizing radiation and leukemia mortality among Japanese atomic bomb survivors, 1950–2000. Radiat Res 2009; 172(3):368–82.
8. Cullings HM, Fujita S, Funamoto S, Grant EJ, Kerr GD, Preston DL. Dose estimation for atomic bomb survivor studies: its evolution and present status. Radiat Res 2006; 166(1):219–54.
9. Preston DL, Ron E, Tokuoka S, Funamoto S, Nishi N, Soda M, et al. Solid cancer incidence in atomic bomb survivors: 1958–1998. Radiat Res 2007; 168(1):1–64.
10. Moloney WC. Leukemia in survivors of atomic bombing. N Engl J Med 1955; 253(3):88–90.
11. Lewis EB. Leukemia and ionizing radiation. Science 1957; 125(3255):965–72.
12. Wald N. Leukemia in Hiroshima City atomic bomb survivors. Science 1958; 127(3300):699–700.
13. Ishimaru T, Hoshino T, Ichimaru M, Okada H, Tomiyasu T. Leukemia in atomic bomb survivors, Hiroshima and Nagasaki, 1 October 1950–30 September 1966. Radiat Res 1971; 45(1): 216–33.
14. Ichimaru M, Ishimaru T, Belsky JL. Incidence of leukemia in atomic bomb survivors belonging to a fixed cohort in Hiroshima and Nagasaki, 1950–71. Radiation dose, years after exposure, age at exposure, and type of leukemia. J Radiat Res (Tokyo) 1978; 19(3):262–82.
15. Pierce DA, Preston DL, Ishimaru T. A method for analysis of cancer incidence in atomic bomb survivors with application to leukemia. Hiroshima: Radiation Effects Research Foundation; 1983.
16. Finch SC, Hrubec Z, Nefziger MD, Hoshino T, Itoga T. Detection of leukemia and related disorders, Hiroshima and Nagasaki; Research plan. Hiroshima: Atomic Bomb Casualty Commission; 1965.
17. Pisciotta AV, Ichimaru M, Tomonaga M. Morphological reviews of peripheral blood and bone marrow of acute and chronic leukemia in atomic bomb survivors. Hiroshima: Radiation Effects Research Foundation; 1984.
18. Matsuo T, Tomonaga M, Bennett JM, Kuriyama K, Imanaka F, Kuramoto A, et al. Reclassification of leukemia among A-bomb survivors in Nagasaki using French-American-British (FAB) classification for acute leukemia. Jpn J Clin Oncol 1988; 18(2): 91–6.
19. Tomonaga M, Matsuo T, Carter RL, Bennett JM, Kuriyama K, Imanaka F, et al. Differential effects of atomic bomb irradiation in inducing major leukemia types (AML, ALL, and CML): Analsyes of open-city cases including Life Span Study cohort cases in atomic bomb survivors based on updated diagnostic systems and the new dosimetry system (DS86). RERF Technical Report no. 9–91: Hiroshima; Radiation Effects Research Foundation; 1991.
20. Bennett J, Catovsky D, Daniel M, Flandrin G, Galton D, Gralnick H, et al. Proposals for the classification of the acute leukaemias. French-American-British (FAB) Co-operative Group. Br J Haematol 1976; 33(4):451–8.
21. Mabuchi K, Soda M, Ron E, Tokunaga M, Ochikubo S, Sugimoto S, et al. Cancer incidence in atomic bomb survivors. Part I: Use of the tumor registries in Hiroshima and Nagasaki for incidence studies. Radiat Res 1994; 137(2 Suppl):S1–16.
22. Fritz AG, Percy C, Jack A, Sobin LH, Parkin MD. International classification of diseases for oncology (ICD-O-3). 3rd ed. Geneva: World Health Organization; 2000.
23. Sposto R, Preston DL. Correcting for catchment area nonresidency in studies based on tumor registry data (RERF CR 1–92). Hiroshima, Japan: Radiation Effects Research Foundation; 1992.
24. Pierce DA, Stram DO, Vaeth M. Allowing for random errors in radiation dose estimates for the atomic bomb survivor data. Radiat Res 1990; 123(3):275–84.
25. Preston DL, Lubin JH, Pierce DA, McConney ME. Epicure Users Guide. Seattle, WA: Hirosoft International Corporation; 1993.
26. Akaike H. A new look at the statistical model identification IEEE Transactions on Automatic Control. 1974; 6:716–23.
27. Richardson DB, Wing S, Schroeder J, Schmitz-Feuerhake I, Hoffmann W. Ionizing radiation and chronic lymphocytic leukemia. Environ Health Perspect 2005; 113(1):1–5.
28. Rericha V, Kulich M, Rericha R, Shore DL, Sandler DP. Incidence of leukemia, lymphoma, and multiple myeloma in Czech uranium miners: a case-cohort study. Environ Health Perspect 2006; 114(6): 818–22.
29. Romanenko AY, Finch SC, Hatch M, Lubin JH, Bebeshko VG, Bazyka DA, et al. The Ukrainian-American study of leukemia and related disorders among Chornobyl cleanup workers from Ukraine: III. Radiation risks. Radiat Res 2008; 170(6):711–20.
30. Linet MS, Schubauer-Berigan MK, Weisenburger DD, Richardson DB, Landgren O, Blair A, et al. Chronic lymphocytic leukaemia: an overview of aetiology in light of recent developments in classification and pathogenesis. Br J Haematol 2007; 139(5): 672–86.
31. United Nations. UNSCEAR. Sources and Effects of Ionizing Radiation: United Nations Scientific Committee on the Effects of Atomic Radiation 2000 Report to the General Assembly, with Scientific Annexes, Vol. II: Effect. United Nations: New York; 2000.
32. United Nations. UNSCEAR. Effects of Ionizing Radiation-UNSCEAE 2006 Report to the General Assembly with Scientific Annexes. Volume I: New York; 2008.
33. Yoshimi I, Mizuno S. Mortality trends of hematologic neoplasms (lymphoma, myeloma, and leukemia) in Japan (1960–2000): with special reference to birth cohort. Jpn J Clin Oncol 2004; 34(10): 634–7.
34. Parkin DM, Whelan SL, Ferlay J, Teppo L, Thomas DB, editors. Cancer incidence in five continents, vol. VIII. IARC Scientific Publications No. 155. Lyon: IARC; 2002.
35. Pierce D, Preston D. Joint analysis of site-specific cancer risks for the atomic bomb survivors. Radiat Res 1993; 134(2):134–42.
36. National Research Council. Health risks from exposure to low levels of ionizing radiation: BEIR VII Phase 2. Washington, DC: National Academies Press; 2006.
37. Muirhead CR, O'Hagan JA, Haylock RG, Phillipson MA, Willcock T, Berridge GL, et al. Mortality and cancer incidence following occupational radiation exposure: third analysis of the National Registry for Radiation Workers. Br J Cancer 2009; 100(1):206–12.
38. Krestinina L, Preston DL, Davis FG, Epifanova S, Ostroumova E, Ron E, et al. Leukemia incidence among people exposed to chronic radiation from the contaminated Techa River, 1953–2005. Radiat Environ Biophys 2010; 49(2):195–201.
39. Nakamura N. A hypothesis: Radiation-related leukemia is mainly attributable to the small number of people who carry pre-existing clonally expanded preleukemic cells. Radiat Res 2005; 163:258–65.
40. Linet M, Cartwright R. The leukemias. In: Schottenfeld D, Joseph F, Fraumeni J, editors. Cancer epidemiology and prevention. 2nd ed. New York: Oxford University Press; 1996. P. 841–92.
41. Iwanaga M, Hsu WL, Soda M, Takasaki Y, Tawara M, Joh T, et al. Risk of myelodysplastic syndromes in people exposed to ionizing radiation: a retrospective cohort study of Nagasaki atomic bomb survivors. J Clin Oncol 2011; 29(4):428–34.
42. Kesminiene A, Evrard A, Ivanov VK, Malakhova IV, Kurtinaitis J,

Stengrevics A, et al. Risk of hematological malignancies among Chernobyl liquidators. Radiat Res 2008; 170(6):721–35.

43. Vrijheid M, Cardis E, Ashmore P, Auvinen A, Gilbert E, Habib RR, et al. Ionizing radiation and risk of chronic lymphocytic leukemia in the 15-Country Study of Nuclear Industry Workers. Radiat Res 2008; 170:661–5.

44. Shilnikova NS, Preston DL, Ron E, Gilbert ES, Vassilenko EK, Romanov SA, et al. Cancer mortality risk among workers at the Mayak nuclear complex. Radiat Res 2003; 159(6):787–98.

45. Tajima K. The 4th nation-wide study of adult T-cell leukemia/lymphoma (ATL) in Japan: estimates of risk of ATL and its geographical and clinical features. The T- and B-cell Malignancy Study Group. Intl J Cancer 1990; 45(2):237–43.

46. Richardson DB, Sugiyama H, Wing S, Sakata R, Grant EJ, Shimizu Y, et al. Positive associations between ionizing radiation and lymphoma mortality among men. Am J Epidemiol 2009; 169(8):969–76.

47. Sont WN, Zielinski JM, Ashmore JP, Jiang H, Krewski D, Fair ME, et al. First analysis of cancer incidence and occupational radiation exposure based on the National Dose Registry of Canada. Am J Epidemiol 2001; 153(4):309–18.

48. Ozasa K, Shimizu Y, Suyama A, Kasagi F, Soda M, Grant EJ, et al. Studies of the mortality of atomic bomb survivors, Report 14, 1950–2003: An overview of cancer and noncancer diseases. Radiat Res 2012; 177(3):229–43.

THE JOURNAL OF BIOLOGICAL CHEMISTRY VOL. 288, NO. 13, pp. 9457–9467, March 29, 2013

Mutations in the Nucleolar Phosphoprotein, Nucleophosmin, Promote the Expression of the Oncogenic Transcription Factor MEF/ELF4 in Leukemia Cells and Potentiates Transformation*

Received for publication, September 3, 2012, and in revised form, February 5, 2013 Published, JBC Papers in Press, February 7, 2013, DOI 10.1074/jbc.M112.415703

Koji Ando[‡], Hideki Tsushima[§], Emi Matsuo[¶], Kensuke Horio[‖], Shinya Tominaga-Sato[**], Daisuke Imanishi[‡], Yoshitaka Imaizumi[§], Masako Iwanaga[‡], Hidehiro Itonaga[‡], Shinichiro Yoshida[¶], Tomoko Hata[§], Ryozo Moriuchi[‡‡], Hitoshi Kiyoi[§§], Stephen Nimer[¶¶], Hiroyuki Mano[‖‖], Tomoki Naoe[§§], Masao Tomonaga[‖], and Yasushi Miyazaki[‡1]

From the [‡]Department of Hematology, Atomic Bomb Disease and Hibakusha Medicine Unit, Nagasaki University Graduate School of Biomedical Sciences, 1-12-4 Sakamoto, Nagasaki, Nagasaki 852-8523, Japan, the [§]Department of Hematology, Nagasaki University Hospital, Nagasaki, Nagasaki 852-8523, Japan, the [¶]Department of Hematology, Nagasaki Medical Center, Omura, Nagasaki 856-0835, Japan, the [‖]Department of Hematology, Japanese Red-Cross Nagasaki Atomic Bomb Hospital, Nagasaki, Nagasaki 852-8104, Japan, the [**]Division of Hematology, Sasebo City General Hospital, Sasebo, Nagasaki 857-8511, Japan, the [‡‡]Department of Internal Medicine, Keijyu Hospital, Isahaya, Nagasaki 854-0121, Japan, the [§§]Department of Hematology and Oncology, Nagoya University Graduate School of Medicine, Nagoya 466-8550, Japan, the [¶¶]Sloan-Kettering Institute, Memorial Sloan-Kettering Cancer Center, New York, New York 10021, and the [‖‖]Division of Functional Genomics, Jichi Medical University, Shimotsuke, Tochigi 329-0498, Japan

Background: MEF/ELF4 can function as an oncogene. We demonstrated the role of MEF/ELF4 in acute myeloid leukemia.
Results: NPM1 inhibited the DNA binding and transcriptional activity of MEF/ELF4 on the HDM2 promoter, whereas NPM1 mutant protein enhanced these activities of MEF/ELF4.
Conclusion: MEF/ELF4 activity may be activated by NPM1 mutant protein.
Significance: NPM1 mutant proteins have a role in MEF/ELF4-dependent leukemogenesis.

Myeloid ELF1-like factor (MEF/ELF4), a member of the ETS transcription factors, can function as an oncogene in murine cancer models and is overexpressed in various human cancers. Here, we report a mechanism by which MEF/ELF4 may be activated by a common leukemia-associated mutation in the nucleophosmin gene. By using a tandem affinity purification assay, we found that MEF/ELF4 interacts with multifactorial protein nucleophosmin (NPM1). Coimmunoprecipitation and GST pull-down experiments demonstrated that MEF/ELF4 directly forms a complex with NPM1 and also identified the region of NPM1 that is responsible for this interaction. Functional analyses showed that wild-type NPM1 inhibited the DNA binding and transcriptional activity of MEF/ELF4 on the HDM2 promoter, whereas NPM1 mutant protein (Mt-NPM1) enhanced these activities of MEF/ELF4. Induction of Mt-NPM1 into MEF/ELF4-overexpressing NIH3T3 cells facilitated malignant transformation. In addition, clinical leukemia samples with NPM1 mutations had higher human MDM2 (HDM2) mRNA expression. Our data suggest that enhanced HDM2 expression induced by mutant NPM1 may have a role in MEF/ELF4-dependent leukemogenesis.

Myeloid ELF1-like factor (MEF/ELF4), a member of the ETS family of transcription factors, is characterized by an 85-amino acid ETS domain that recognizes a core sequence of GGAA or TTCC (1). MEF/ELF4 is expressed in various normal and malignant hematopoietic cells and regulates the expression of various cytokines (interleukin-3 (1), granulocyte-macrophage colony-stimulating factor (1), and interleukin-8 (2) as well as the cytolytic perforin molecule (3) and antibacterial peptides lysozyome and human β-defensin2 (4)) and matrix metalloproteinase-9 expression (5). Furthermore, analyses of MEF/ELF4-deficient mice have revealed the essential role of MEF/ELF4 in the development and function of NK (natural killer) cells and NK-T cells (3). Recently, Smith *et al.* (6) have shown that repression of Elf-4 by transcriptional repressor *Gfi1b* is important for the maturation of primary fetal liver erythroid cells. MEF/ELF4 also regulates the key aspects of hematopoietic stem cell behavior by controlling movement through the cell cycle from quiescence (G_0) to G_1 and from G_1 to S as well as resistance to myelosuppression (7, 8).

MEF/ELF4 is expressed in cancers such as leukemia (9), lymphoma, and ovarian cancer (10). Recently, Totoki *et al.* (11) identified an intrachromosomal inversion (Xq25) in hepatocellular carcinoma that generated a BCORL1-MEF/ELF4 fusion transcript. Experiments in several mouse models have suggested that MEF/ELF4 plays a role in tumorigenesis. For example, models of retrovirus-induced insertional mutagenesis have identified *MEF/ELF4* as a gene that is involved in leukemic transformation (12). Sashida *et al.* (13) have shown that overexpression of MEF/ELF4 enhances the expression of Mdm2,

* This work was supported in part by a grant from the Ministry of Health, Welfare, and Labor and a grant from the Ministry of Education, Culture, Sports, Science, and Technology of Japan.
[1] To whom correspondence should be addressed. Tel.: 81-95-819-7111; Fax: 81-95-819-7113; E-mail: y-miyaza@nagasaki-u.ac.jp.

leading to decreased p53 expression and enhanced transformation. In experiments with MEF/ELF4-overexpressing cells, they demonstrated that Ets1-induced p16 induction is suppressed, resulting in senescence suppression and tumor promotion.

Nucleophosmin (NPM1) is a nucleolar phosphoprotein (14) and a frequent target of genetic alterations in hematopoietic malignancies. *NPM1* gene mutations have been found in ~60% of adult patients who have acute myeloid leukemia (AML)[2] and a normal karyotype (15). These mutations lead to the aberrant cytoplasmic expression of NPM1 ($NPMc^+$) due to nucleotide gain at the C terminus (16, 17), which results in the loss of tryptophan residues essential for nucleolar localization and the gain of a new nuclear export signal (18). Increased NPM1 export into the cytoplasm probably perturbs multiple cellular pathways by delocalizing the proteins that interact with NPM1. By using a transgenic mouse model expressing the human $NPMc^+$ mutation, it has been shown that $NPMc^+$ confers a proliferative advantage in the myeloid lineage, suggesting that NPM1 mutations can participate in leukemia development (19).

In the present study, we found that wild-type NPM1 (Wt-NPM1) down-regulates, whereas mutated NPM1 (Mt-NPM1) up-regulates, the transcriptional activity of MEF/ELF4 on the human MDM2 (HDM2) promoter. The expression of Mt-NPM1 in MEF/ELF4-overexpressing NIH3T3 cells resulted in enhanced malignant transformation. We also found that *HDM2* mRNA expression in primary AML cells with *NPM1* mutations is significantly higher compared with AML cells without *NPM1* mutations. Taken together, our data suggest that *NPM1* mutations may promote transformation by enhancing the oncogenic functions of MEF/ELF4.

EXPERIMENTAL PROCEDURES

Cell Culture—293T cells (CRL-11268, ATCC (Manassas, VA)) were maintained at 37 °C in DMEM (Invitrogen) with bovine calf serum. U937 cells (CRL-1593.2, ATCC) were maintained with 10% (v/v) FBS, 100 IU/ml penicillin, and 100 μg/ml streptomycin (Fisher). NIH3T3 cells (CRL-1658, ATCC) were maintained under identical conditions with 10% (*v/v*) FBS and grown in RPMI 1640 (Fisher) with 10% FCS (HyClone, Logan, UT), 100 units/ml penicillin G, and 100 μg/ml streptomycin. COS7 cells (CRL-1651, ATCC) were cultured in DMEM (Invitrogen) containing 10% FCS.

Tandem Affinity Purification Assay—The cDNA of MEF/ELF4 was inserted into InterPlay N-terminal mammalian TAP vector (pTAP/MEF/ELF4, Stratagene (San Diego, CA)) comprising two affinity tags (immunoglobulin G (IgG)-binding domain and calmodulin-binding peptide) separated by the cleavage site of tobacco etch virus protease (20). 293T cells were transfected with pTAP or pTAP/MEF/ELF4 plasmids in a 10-cm dish. Transfected cells were collected and lysed in a solution containing 100 mM Tris-HCl (pH 8.0), 300 mM NaCl, and 0.1% Nonidet P-40. The lysate was centrifuged at 15,000 rpm for 30 min at 4 °C. The resulting supernatant was incubated for 2 h at 4 °C with IgG-Sepharose 6 Fast Flow (GE Healthcare), after which the resin was washed and incubated with tobacco etch virus protease for 2 h at 16 °C. Purification on calmodulin affinity resin (Stratagene) was performed according to the manufacturer's instructions. Purified proteins were precipitated with trichloroacetic acid, resolved with 1× sample buffer and subjected to SDS-PAGE. Gels were stained with Coomassie Blue, and protein bands were cut out. Proteins were eluted with trypsin. The resulting peptides were analyzed with a Procise 49X cLC protein sequencer (Applied Biosystems, Foster City, CA) (20).

In Vitro Translation—The cDNA molecules of Wt-NPM1 and Mt-NPM1 (21) were inserted into the pTnT vector (pTnT-NPM, Promega (Madison, WI)) for *in vitro* translation. NPM1 protein (biotin-NPM1) was *in vitro*-translated with pTnT-NPM1 and labeled with biotinylated lysine (Transcend tRNA, Promega) by using the TNT Quick Coupled transcription/translation system (Promega). The cDNA of MEF/ELF4 was inserted into pET-3a (Novagen, VWR (Lisbon, Portugal)), which allows the introduction of a His tag into the N terminus of MEF/ELF4 (pET/MEF/ELF4). Overexpression of the recombinant protein (His-MEF/ELF4) was achieved in *Escherichia coli* BL21Gold (DE3) cells (Stratagene) transformed with the constructed plasmid pET/MEF/ELF4. His-MEF/ELF4 was isolated from cells broken in lysis buffer (STE buffer) with sonication and centrifuged at 15,000 × *g* for 10 min at 4 °C (1).

Biotin-NPM1 was incubated with His-MEF/ELF4 or His (as a control) proteins at 4 °C for 1 h. The mixture was loaded onto His spin traps (GE Healthcare) and eluted with 500 mM imidazole at pH 7.4. After SDS-PAGE and electroblotting, biotin-NPM1 in purified samples was detected by using the Transcend non-radioactive translation detection system (Promega).

Immunoprecipitation and Immunoblotting—MEF/ELF4 was cloned into p3xFLAG-CMV (Sigma) (FLAG-MEF/ELF4) from PCR products generated from pcDNA/MEF/ELF4 (1). Wt-NPM1 and Mt-A-NPM1 were cloned into pcDNA3.1/V5-His (pcDNA/V-Wt-NPM1 and Mt-A-NPM1, respectively) (Invitrogen) from PCR products generated from pcDNA/Wt-NPM1 and pcDNA/Mt-A (21). 293T cells were transfected with each plasmid by using Effectene transfection reagent (Qiagen, Berlin, Germany). After 48 h, cells were lysed by using the Universal Magnetic co-immunoprecipitation kit (Active Motif, Carlsbad, CA) following the manufacturer's instructions for nuclear extraction. Lysates were centrifuged at 15,000 rpm for 10 min at 4 °C to remove the resin. The resulting supernatants were incubated for 4 h at 4 °C with 5 μg of antibodies against FLAG (Sigma), 5 μg of antibodies against V5 (Invitrogen), or normal mouse IgG (Santa Cruz Biotechnology, Inc., Santa Cruz, CA).

Immunoprecipitates were recovered, washed four times with ice-cold co-immunoprecipitation solution (Active Motif), and fractionated by SDS-PAGE. Separated proteins were transferred to a membrane. After incubation in blocking buffer, membranes were probed with peroxidase-labeled antibodies against FLAG (Sigma), V5 (Invitrogen), or tag (Invitrogen). Detection was achieved with an enhanced chemiluminescence system (ECL Advance Western blotting detection kit, GE Healthcare). Quantification of Western blotting bands was per-

[2] The abbreviations used are: AML, acute myeloid leukemia; Wt-NPM1, wild type NPM1; Mt-NPM1, mutant NPM1; RQ-PCR, quantitative reverse transcription-polymerase chain reaction.

formed by using AE-6982/C/FC and CS Analyzer version 3.0 software (ATTO, Tokyo, Japan).

GST and His Pull-down Assay—Fusion protein of GST and Wt-NPM1 (GST-NPM1) and GST-NPM1 deletion mutant constructs (Fig. 1*C*) were generated by PCR with pcDNA/Wt-NPM1 as a template. PCR products were cloned in-frame into bacterial expression vector pGEX-T4. Plasmids that express GST fusion protein (GST-NPM1, GST-NPM1 deletion mutants) and His-MEF/ELF4 protein (pET/MEF/ELF4) or their controls were transfected into *E. coli*. Bacterial pellets were lysed in 1 ml of phosphate-buffered saline (PBS) with sonication. His-MEF/ELF4 or His alone was incubated with an equivalent amount of GST, GST-Wt-NPM1, or GST-Wt-NPM1 deletion mutants for 1 h at 4 °C. Proteins were purified by using GST columns (MicroSpin GST Purification Module, GE Healthcare) or His columns. Bound proteins were analyzed by using SDS-PAGE/immunoblot.

EMSA—Recombinant proteins GST, GST-NPM1, His, and His-MEF/ELF4 were collected as described above. Nuclear protein from 293T cells transfected with pcDNA/MEF/ELF4, pcDNA/Wt-NPM1, or pcDNA/Mt-A-NPM1 was extracted with the NE-PER nuclear and cytoplasmic extraction kit (Pierce) according to the manufacturer's instructions. EMSA was performed by using the LightShift chemiluminescent EMSA kit (Pierce). Recombinant protein or nuclear extracts were incubated with 20 fmol of biotin 3′-end-labeled oligonucleotides containing APET (an ETS binding site in the IL-3 promoter that was shown to bind to MEF/ELF4) (1). After electrophoresis, transfer, and cross-linking, the signal was detected by a peroxidase/luminol system (chemiluminescent nucleic acid detection module, Pierce). To confirm specificity, a 200-fold excess amount of non-labeled oligonucleotides (APET competitor) (1) was added. The DNA sequence of the APET oligonucleotide is 5′-CCTCAGTGAGCTGAGTCAGG-CTTCCCCTTCCTGCCACAGGG-3′.

RNA Interference—siRNA for NPM1 was transfected into 293T cells by using the GeneClip U1 hairpin cloning system (Promega) according to the manufacturer's instructions. The siRNA sequence-targeting NPM1 gene corresponded to nucleotides 103–125 of the coding region relative to the first nucleotide of the start codon, as described previously (22).

Luciferase Assay—A 0.5-μg aliquot of pcDNA/MEF/ELF4, pcDNA/Wt-NPM1, pcDNA/Mt-A-NPM1, pcDNA/Mt-I-NPM1, or pcDNA/Mt-J-NPM1 was transfected into U937, 293T, and COS7 cells seeded in 6-well dishes by using Nucleofectin (Qiagen) together with 0.1 μg of pGL4 reporter plasmid (pGL4/APET (1), pGL4/ETSm-APET (1), pGL4/HDM2, or pGL4/HDM2mut) and 0.05 μg of pLR-Bact vector. pGL4/ETSm-APET contains a mutation in the ETS binding site (ETSm-APET, 5′-CCTCAGTGAGCTGAGTCAGGCTgagC-CTcgacGCCACAGGG-3′). pGL4/HDM2 contains a wild-type hdm2 (P2) promoter sequence from bp −82 to −122 (Wt-Ets, CAGGTTGACTCAGCTTTTCCTCTTGAGCTGGTCAAG-TTCAG), and pGL4/HDM2mut contains an hdm2 (P2) promoter sequence with a mutated ETS site (Mt-Ets, CAGGTTG-ACTCAGCTTTTaCTCTTGAGCTGGTCAAGTTCAG) (23). Cell lysates were prepared 48 h after transfection, and luciferase activity was determined by using the Dual-Luciferase reporter assay system (Promega).

Anchorage-independent Growth Assay—NIH3T3 cells were plated on 24-well dishes in soft agar containing DMEM supplemented with 10% FCS after they were transfected with various combinations of empty vector, pcDNA/MEF/ELF4, pcDNA/Wt-NPM1, or pcDNA/Mt-A-NPM1 and cultured for 2 weeks. Images were taken with a Leica DM IRBE inverted microscope (Leica Microsystems GmbH, Mannheim, Germany) with a ×10 objective lens.

Immunochemistry—MEF/ELF4 was cloned into the pGFP-C3 vector (Clontech, Mountain View, CA) (pGFP-MEF/ELF4). 293T cells were transfected with the empty vector, pGFP-MEF/ELF4, pcDNA/V-Wt-NPM1, or pcDNA/V-Mt-A-NPM1. Cells were harvested 3 days after transfection. Cytospin samples were fixed for 15 min in PBS containing 4% paraformaldehyde. Fixed coverslips were washed twice in TBS, permeabilized in 0.5% Triton X-100 for 10 min, and incubated in Image-iT FX signal enhancer (Invitrogen) for 30 min. Cells were incubated with primary antibody for 1 h and then washed extensively in TBS before incubation with Alexa546-conjugated goat anti-mouse-IgG antibody (dilution 1:2000; Invitrogen) for 1 h. Cells were covered with a drop of ProLong Gold Antifade Reagent with DAPI (Invitrogen). Fluorescent images were obtained by using a confocal laser-scanning microscope (LSM 5 Pascal V3.2, Carl Zeiss).

ChIP Assay—293T cells were transfected with empty vector, pcDNA/MEF-FLAG, pcDNA/Wt-NPM1, or pcDNA/Mt-A-NPM1 by using a nucleofection kit (Qiagen). After 48 h of culture at 26 °C, cells were fixed by the addition of 1% formaldehyde in PBS for 10 min. Chromatin isolation and shearing were performed by using the OneDay ChIP kit (Diagenode, Liege, Belgium) and Shearing-ChIP kit (Diagenode) according to the manufacturer's instructions. Immunoprecipitation reactions were performed with anti-FLAG monoclonal antibody (Sigma) or isotype control IgG (BD Biosciences). Samples were analyzed by quantitative reverse transcription-polymerase chain reaction (RQ-PCR) by using the LightCycler DNA Master SYBR Green I kit (Roche Applied Science) as specified by the manufacturer. The primer sequences for the HDM2 promoter were 5′-GAACGCTGCGCGTAGTCTGG-3′ (forward) and 5′-ACTGC-AGTTTCGGAACGTGT-3′ (reverse).

Clinical Samples—Informed consent for sample collection was obtained according to protocols approved by the International Review Board of Nagasaki University, Nagasaki, Japan (approval number 33-3). Bone marrow aspirates were collected from 22 AML patients before the initiation of chemotherapy. CD34-positive cells were isolated by using Ficoll density gradient centrifugation and magnetic beads (CD34 Isolation Kit, Miltenyi Biotec, Auburn, CA) to minimize the confounding effect of MEF/ELF4 and NPM1 expression by mature myeloid cells. For the screening of *NPM1* mutations, genomic DNA corresponding to exon 12 was amplified by using forward primer 5′-TTAACTCTCTGGTGGTAGAATGAA-3′ and reverse primer 5′-CAAGACTATTTGCCATTCCTAAC-3′, as reported previously. Amplified products were separated by agarose gel electrophoresis, purified by using a QIAquick gel extraction kit (Qiagen), and directly sequenced by using a DNA sequencer

(3100, Applied Biosystems) with the BigDye terminator cycle sequencing kit (Applied Biosystems). When mutations were found by direct sequencing, the fragments were cloned into a pTOPO vector (Invitrogen) and then transfected into the *E. coli* strain DH5A. At least four recombinant colonies were selected, and plasmid DNA samples were prepared by using the QIAprep Spin Miniprep kit (Qiagen). Cloned fragments were sequenced to confirm the mutation of the *NPM1* gene.

Total RNA was harvested from purified CD34-positive cells by using an RNeasy minikit (Qiagen). cDNA synthesis was undertaken by using an oligo(dT) primer with the PrimeScript II first strand cDNA synthesis kit (Takara, Shiga, Japan). These cDNA molecules were measured by RQ-PCR with the primers listed under "RQ-PCR."

RQ-PCR—RQ-PCR was performed by using a LightCycler TaqMan Master kit (Roche Applied Science) following the manufacturer's instructions. Twenty microliters of Universal ProbeLibrary probes (Exiqon, Vedbaek, Denmark) were added in the final reaction. Primers designed by using the Universal ProbeLibrary Assay Design Centre (available on the Roche Applied Science Web site) were synthesized by Sigma. PCR amplification was performed by using a LightCycler 350S instrument (Roche Applied Science). Thermal cycling conditions comprised 2 min at 40 °C and 10 min at 95 °C, followed by 45 amplification cycles at 95 °C for 10 s, 60 °C for 30 s, and 72 °C for 1 s and then a 40 °C cooling cycle for 30 s. Specific primers and probes were as follows: for *HDM2*, forward (5′-TCTGATAGTATTTCCCTTTCCTTTG-3′), reverse (5′-TGTTCACTTACACCAGCATCAA-3′), and probe (5′-CGCCACTTTTTCTCTGCTGATCCAGG-3′); for human *MEF/ELF4*, forward (5′-TGGAGACTCTCAGGGTCGAAA-3′), reverse (5′-AAGCAACGGGATGGATGAT-3′), and probe (5′-TCACAGCTGGGAACACAGAG-3′); and for human *G6PDH*, forward (5′-AAGCAACGGGATGGATGAT-3′), reverse (5′-TCACAGCTGGGAACACAGAG-3′), and probe (5′-CGCCACTTTTTCTCTGCTGATCCAGG-3′).

Statistical Analyses—Comparisons of patient characteristics between two groups were performed with the Wilcoxon test. The results of *in vivo* experiments are presented as the mean ± S.D. of three independent experiments and compared by using one-way analysis of variance followed by Scheffe's multiple comparison test. A p value of 0.05 was considered statistically significant.

RESULTS

Identification of MEF/ELF4-binding Protein—To identify the proteins that bind to MEF/ELF4, we performed the tandem affinity purification (TAP) procedure and analyzed the amino acid sequence of the protein complex, thereby identifying 25 proteins (including NPM1). NPM1 is essential for embryonic development and is frequently translocated or mutated in hematological malignancies (24). Therefore, we decided to focus on the interaction between NPM1 and MEF/ELF4.

Wt-NPM1 Interacts with MEF/ELF4 in Vivo and in Vitro—To determine if Wt-NPM1 interacts with MEF/ELF4 in human cells, we transfected 293T cells with FLAG-MEF/ELF4 and V5-Wt-NPM1 expression plasmids and performed immunoprecipitations with mouse monoclonal anti-FLAG or anti-V5 antibody. As shown in Fig. 1*A*, FLAG-MEF/ELF4 protein co-precipitated with V5-Wt-NPM1 by the anti-V5 antibody (*lane 1*) but not by the isotype-matched control (*lane 2*). In reciprocal experiments, V5-Wt-NPM1 protein co-precipitated with FLAG-MEF/ELF4 protein by the anti-FLAG antibody (*lane 3*). These results showed the *in vivo* interaction between Wt-NPM1 and MEF/ELF4. To ascertain whether Wt-NPM1 protein interacted directly with MEF/ELF4, an *in vitro* association assay with biotin-labeled *in vitro*-translated Wt-NPM1 and bacterially recombinant His-MEF/ELF4 fusion protein was performed (Fig. 1*B*). Biotin-labeled Wt-NPM1 bound to His-MEF/ELF4 (*lane 1*) but not to His alone (*lane 2*). These results demonstrated that His-MEF/ELF4 bound directly to Wt-NPM1.

To characterize the region of Wt-NPM1 that binds MEF/ELF4, five distinct GST-NPM1 proteins were prepared (Fig. 1*C*). GST pull-down assays (Fig. 1*D* (*a*)) and His tag pull-down assays (Fig. 1*D* (*b*)) revealed that the N-terminal region of NPM1 (the F1, F2, and F3 fragments that contain the oligomerization domain) bound to His-MEF/ELF4, unlike the C-terminal region of NPM1 (F4 and F5).

Wt-NPM1 Interferes with MEF/ELF4 Binding to Target DNA Sequences—To assess the direct role of Wt-NPM1 in MEF/ELF4 action, we undertook EMSA. His-MEF/ELF4 bound to the APET probe (1), but no band was observed with His, GST, or GST-NPM1 (Fig. 2). The shifted band of MEF/ELF4 was diminished when the APET competitor was added to the reaction mixture. When Wt-NPM1 was added to the reaction mixture, the shifted band containing MEF/ELF4 was diminished. These results implied that Wt-NPM1 inhibits the DNA binding of MEF/ELF4 DNA through direct interactions.

Wt-NPM1 Inhibits, whereas Mt-NPM1 Enhances, MEF/ELF4-dependent Transcriptional Activity—To study the functional relevance of the physical interaction between MEF/ELF4 and Wt-NPM1, we transfected pcDNA/MEF/ELF4 in combination with pcDNA/Wt-NPM1 and examined the activity of the APET promoter construct (1) in 293T cells (Fig. 3*A*). As reported previously, MEF/ELF4 activated the APET promoter by ~159-fold. Co-expression of Wt-NPM1 with MEF/ELF4 led to a significant decrease in luciferase activity. Similar data were obtained by using COS7 cells (Fig. 3*B*) and a human leukemia cell line, U937 (Fig. 3*C*).

Having shown that NPM1 expression attenuated the transcriptional activity of MEF/ELF4 in leukemia cells, we next assessed whether the inhibition of Wt-NPM1 expression *in vivo* enhanced MEF/ELF4-dependent transcriptional activity. The siRNA directed against Wt-NPM1 in 293T cells suppressed the expression of Wt-NPM1 protein by 60–70% (Fig. 3*D*). Transient transfections were performed by using NPM1-knockdown 293T cells with pcDNA/MEF/ELF4 and pGL4/APET reporter plasmids. A luciferase assay revealed that MEF/ELF4-dependent transcriptional activity was significantly elevated in Wt-NPM1-knockdown cells by 1.8-fold (Fig. 3*E*). These results implied that Wt-NPM1 functioned as an inhibitor of MEF/ELF4.

Mutated nucleophosmin (Mt-NPM1) has been found in 50% of adult AML patients with normal karyotypes (15). It has been suggested that the mutation is a critical event for leukemogen-

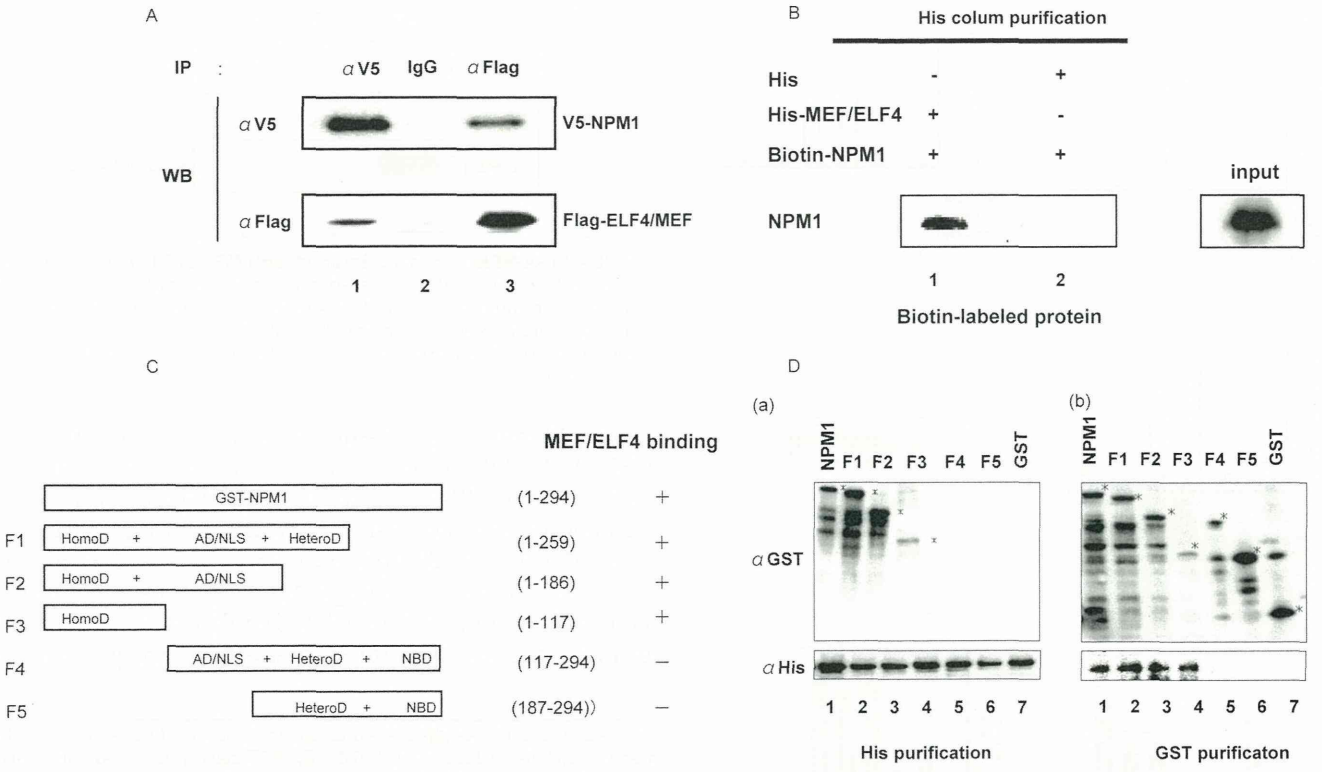

FIGURE 1. **NPM1 interacts with MEF/ELF4.** *A*, 293T cells were transfected with the indicated expression plasmids. After 48 h, cell lysates were immunoprecipitated (*IP*) with anti-FLAG and anti-V5 antibodies. Immunoprecipitates were analyzed by 10% SDS-PAGE and subjected to immunoblotting (*WB*) with anti-V5 antibody (*top row*) or anti-FLAG antibody (*bottom row*). *B*, MEF/ELF4 interacts directly with NPM1 *in vitro*. *In vitro* association assays were undertaken by incubating His-MEF/ELF4 fusion protein immobilized by using a His-column with biotin-labeled MEF/ELF4 (*lane 1*). His alone was incubated with biotin-labeled NPM1 (*lane 2*) as a control. *C*, NPM1 structure and the relative binding of MEF/ELF4 (*schematic*). *HomoD*, homodimerization domain, residues 1–117; *AD/NLS*, acidic domain/nuclear localization sequence, residues 117–187; *HeteroD*, heterodimerization domain, residues 187–259; *NBD*, nucleic acid binding domain, residues 259–294. *D*, the N-terminal portion of NPM1 is the MEF/ELF4-interacting domain. Bacterially expressed and purified GST, GST-NPM1, and GST-NPM1 mutants with deletions were mixed with bacterially expressed and purified His or His-MEF/ELF4 protein. Recombinant proteins were subjected to His or GST affinity columns, followed by immunoblotting with anti-GST or anti-His antibodies. *a*, the reactive samples were subjected to analyses on a His affinity column followed by immunoblotting with anti-His antibodies (*bottom left*) or with anti-GST antibodies (*top left*). *b*, the reactive samples were subjected to GST affinity columns, followed by immunoblotting with anti-GST antibodies (*top right*) or with anti-His antibodies (*bottom right*).

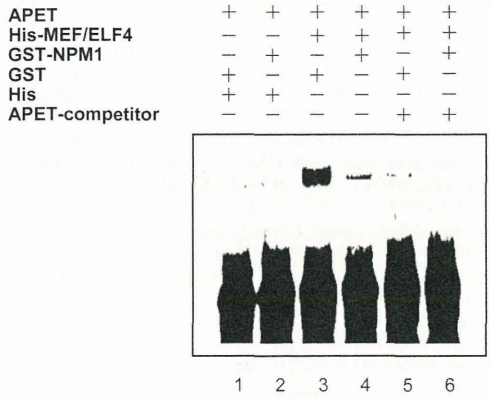

FIGURE 2. **EMSA with recombinant His-MEF/ELF4, His, GST, and GST-Wt-NPM1.** His-MEF/ELF4 was incubated with GST and GST-Wt-NPM1 at room temperature prior to EMSA by using a biotin-conjugated APET probe (*lanes 1–4*). An excess amount of unlabeled APET competitor was added to the reaction mixtures (*lanes 5* and *6*).

esis. To determine the effect of Mt-NPM1 on the transcription-activating properties of MEF/ELF4, we transfected pcDNA/MEF/ELF4 in combination with pcDNA/Mt-A-NPM1, pcDNA/Mt-I-NPM1, or pcDNA/Mt-J-NPM1 and then examined the activity of the APET promoter construct in 293T cells (Fig. 3*F*). Co-expression of Mt-NPM1 with MEF/ELF4 led to a 315-fold increase in luciferase activity. Similar data were obtained with COS7 (Fig. 3*G*) and U937 (Fig. 3*H*) cells. To show the effect of the coexistence of both Wt- and Mt-NPM1, we transfected 293T cells with various amounts of plasmids that expressed Wt-NPM1 and Mt-A-NPM1. The expression of Mt-NPM1 enhanced MEF/ELF4-dependent APET promoter activation in a dose-dependent manner, even in the presence of Wt-NPM1 (Fig. 3*I*). Taken together, our results suggest that Wt-NPM1 has an inhibitory effect, whereas Mt-NPM1 has enhancing effect, on the function of MEF/ELF4.

Mt-NPM1 Does Not Interact with MEF/ELF4 in Vivo—Because the mutated region of Mt-NPM1 was located outside the domain responsible for interaction with MEF/ELF4, we hypothesized that Mt-NPM1 might bind to MEF/ELF4. To test this hypothesis, we transfected 293T cells with FLAG-MEF/ELF4 and V5-Mt-A-NPM1 expression plasmids and performed immunoprecipitations with mouse monoclonal anti-FLAG or anti-V5 antibody. Contrary to our expectations, as shown in Fig. 4, FLAG-MEF/ELF4 protein and V5-Wt-A-NPM1 did not co-precipitate with each other (Fig. 4). These results showed that there is little *in vivo* interaction between Mt-A-NPM1 and MEF/ELF4.

Localization of MEF/ELF4 Is Unaffected by Mt-NPM1—Having shown that Mt-NPM1 enhances the transcriptional activity of MEF/ELF4, we next assessed whether Mt-NPM1 dislocates

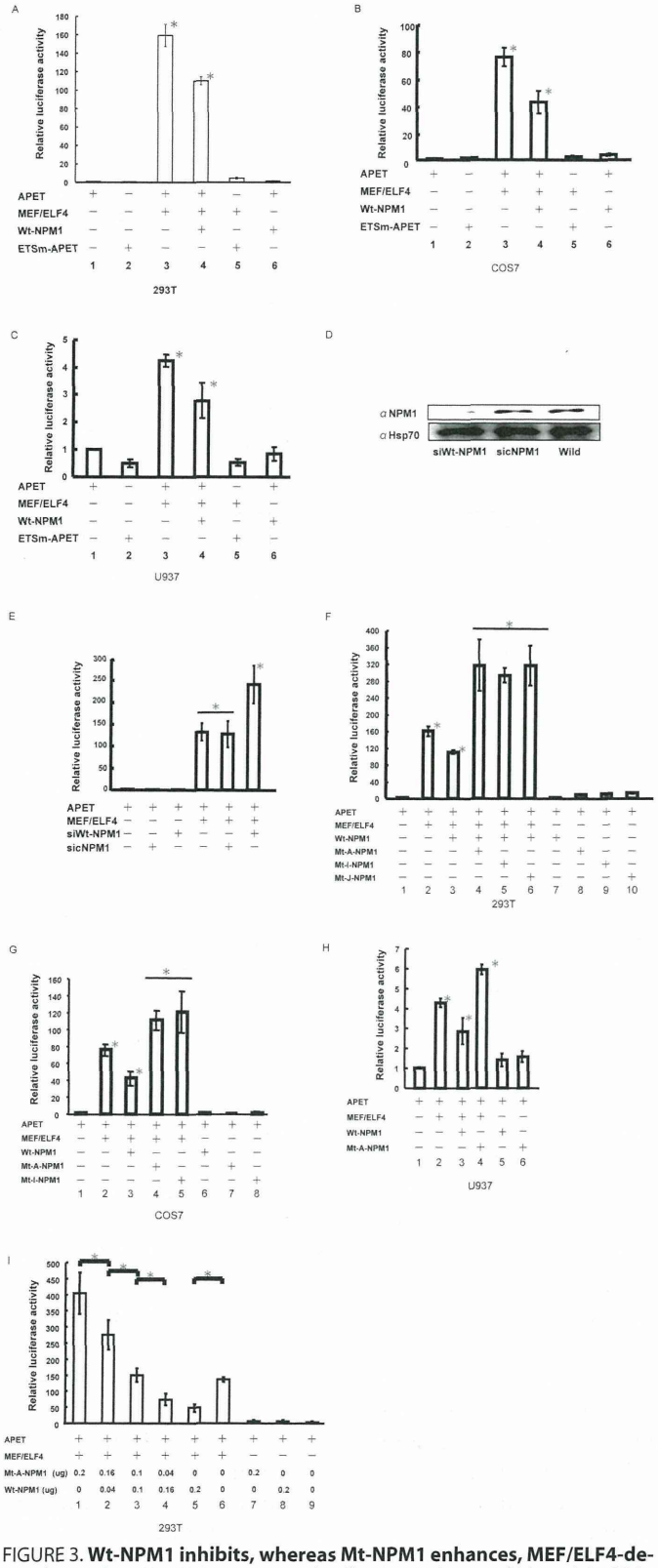

FIGURE 3. **Wt-NPM1 inhibits, whereas Mt-NPM1 enhances, MEF/ELF4-dependent APET promoter transactivation.** 293T human kidney (*A*), COS7 monkey kidney (*B*), and U937 human hematological (C) cell lines were co-transfected with the luciferase reporter gene of an artificial MEF/ELF4 target promoter (APET) and effector genes. The target promoter and effector genes were as follows: pGL4/APET (*lane 1*); pGL4/ETSm-APET (*lane 2*); pGL4/APET and pcDNA/MEF/ELF4 (*lane 3*); pGL4/APET, pcDNA/MEF/ELF4, and pcDNA/Wt-NPM1 (*lane 4*); pGL4/ETSm-APET and pcDNA/MEF/ELF4 (*lane 5*); and pGL4/APET and pcDNA/Wt-NPM1 (*lane 6*). Luciferase activity by pGL4/APET alone was assigned a value of 1.0. The analysis was performed in triplicate assays, and the results were reproducible. The results are shown as the mean ± S.D. (*error bars*). *, $p < 0.05$. *D*, 293T cells transduced with siRNA encoding vector (siWt-NPM1) were harvested 72 h after transduction for Western blotting. Hsp90 is shown as a control. *sicNPM1*, control siRNA non-relevant to the expression of NPM1; *Wild*, without transduction. *E*, 293T cells were co-transfected with the luciferase reporter plasmid (pGL4/APET), expression plasmid (pcDNA MEF/ELF4), and siWt-NPM1 gene (pcDNA/siRNA-Wt-NPM1) or control. Luciferase activity by pGL4/APET alone was assigned a value of 1.0. The analysis was performed in triplicate assays, and the results were reproducible. The results are shown as the mean ± S.D. *, $p < 0.05$. *F*, 293T cells were co-transfected with the luciferase reporter gene of an artificial MEF/ELF4 target promoter and effector genes. Target promoter and effector genes were as follows: pGL4/APET (*lane 1*); pGL4/APET and pcDNA/MEF/ELF4 (*lane 2*); pGL4/APET, pcDNA/MEF/ELF4, and Wt-NPM1 (*lane 3*); pGL4/APET, pcDNA/MEF/ELF4, and Mt-A-NPM1, Mt-I-NPM1, or Mt-J-NPM1 (lanes 4–6, respectively); and pGL4/APET and pcDNA/Wt-NPM1, Mt-A-NPM1, Mt-I-NPM1, or Mt-J-NPM1 (lanes 7–10, respectively). Luciferase activity by pGL4/APET alone was assigned a value of 1.0. The analysis was performed in triplicate assays, and the results were reproducible. The results are shown as the mean ± S.D. *, $p < 0.05$. *G*, COS7 cells were co-transfected with the luciferase reporter gene of an artificial MEF/ELF4 target promoter and effector genes. The target promoter and effector genes were as follows: pGL4/APET (*lane 1*); pGL4/APET and pcDNA/MEF/ELF4 (*lane 2*); pGL4/APET, pcDNA/MEF/ELF4, and Wt-NPM1 (*lane 3*); pGL4/APET, pcDNA/MEF/ELF4, and Mt-A-NPM1 or Mt-I-NPM1 (*lanes 4* and *5*, respectively); and pGL4/APET and pcDNA/Wt-NPM1, Mt-A-NPM1, or Mt-I-NPM1 (*lanes 6–8*, respectively). Luciferase activity by pcDNA/APET alone was assigned a value of 1.0. The analysis was performed in triplicate assays, and the results were reproducible. The results are shown as the mean ± S.D. (*, $p < 0.05$). *H*, U937 cells were co-transfected with the luciferase reporter gene of an artificial MEF/ELF4 target promoter and effector genes. Target promoter and effector genes were as follows: pGL4/APET (*lane 1*); pGL4/APET and pcDNA/MEF/ELF4 (*lane 2*); pGL4/APET, pcDNA/MEF/ELF4, and Wt-NPM1 (*lane 3*); pGL4/APET, pcDNA/MEF/ELF4, and Mt-A-NPM1 (*lane 4*); and pGL4/APET and pcDNA/Wt-NPM1 or Mt-A-NPM1 (*lanes 5* and *6*, respectively). Luciferase activity by pcDNA/APET alone was assigned a value of 1.0. The analysis was performed in triplicate assays, and the results were reproducible. The results are shown as the mean ± S.D. *, $p < 0.05$. *I*, 293T cells were co-transfected with 0.1 μg of the luciferase reporter gene of an artificial MEF/ELF4 target promoter (*lanes 1–9*) and 0.1 μg of effector genes (pcDNA/MEF/ELF4) (*lanes 1–6*). The effector genes were as follows: 0.2 μg of Mt-A-NPM1 (*lane 1*); 0.16 μg of Mt-A-NPM1 and 0.04 μg of Wt-NPM1 (*lane 2*); 0.1 μg of Mt-A-NPM1 and 0.1 μg of Wt-NPM1 (*lane 3*); 0.04 μg of Mt-A-NPM1 and 0.16 μg of Wt-NPM1 or 0.2 μg of Wt-NPM1 (*lanes 4 and 5*, respectively); none (*lane 6*); pGL4/APET and 0.2 μg of Mt-A-NPM1 (*lane 7*); pGL4/APET and 0.2 μg of Wt-NPM1 (*lane 8*); and pGL4/APET (*lane 9*). Luciferase activity by pGL4/APET alone was assigned a value of 1.0. The analysis was performed in triplicate assays, and the results were reproducible. The results are shown as the mean ± S.D. *, $p < 0.05$.

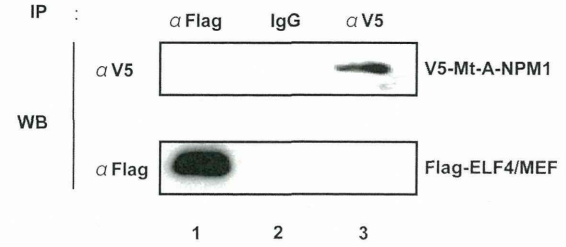

FIGURE 4. **Mt-A-NPM1 does not interact with MEF/ELF4 *in vivo*.** 293T cells were transfected with the indicated expression plasmids. After 48 h, cell lysates were immunoprecipitated (*IP*) with anti-FLAG and anti-V5 antibodies. Immunoprecipitates were analyzed by 10% SDS-PAGE and subjected to immunoblotting (*WB*) with anti-V5 antibody (*top row*) or anti-FLAG antibody (*bottom row*).

MEF/ELF4 into the cytoplasm. We transiently co-transfected a MEF/ELF4-GFP fusion protein vector together with the pcDNA/V-Wt-NPM1 or pcDNA/V-Mt-A-NPM1 expression vector into 293T cells. Wt-NPM1 protein and MEF/ELF4 localized to the nucleus (Fig. 5*A* (*a*)), whereas Mt-A-NPM1 protein localized to the cytoplasm (Fig. 5*A* (b)). Contrary to our expectations, the presence of Mt-A-NPM1 did not affect the subcellular distribution of MEF/ELF4. Western blot analysis of MEF/